



Decontamination of Heavy Metals from Soil by Electrokinetic Combined with Reactive Filter Media from Industrial Wastes

Faris M. Hamdi · Ali Altaee · Yahia Aedan · John Zhou · Maryam AL-Ejji · Alaa H. Hawari · Syed Javaid Zaidi · Marwa Mohsen · Rokhsare Kardani

Received: 11 February 2025 / Accepted: 24 May 2025
© Crown 2025

Abstract The electrokinetic (EK) is an in-situ method for soil remediation, aiming to reduce extensive excavation and mitigate risks associated with exposure to hazardous substances. However, heavy metal precipitation near the cathode under alkaline pH remains challenging. This study employed recyclable waste materials of sawdust crosslinked by glutaraldehyde with iron slag as a reactive filter media (RFM) for single and mixed heavy metals from kaolinite and natural soils. Experiments were conducted over two and three weeks, employing 20 to 30 mA electric currents. Incorporating iron slag RFM into the EK process resulted in a notable enhancement in copper removal

from 3.21% to 23.76%. Mixing sawdust with iron slag in the RFM further improved the efficiency of copper extraction from the soil, reaching 71.80%. Also, copper removal improved as the electric current increased from 20 to 25 mA, reaching 88.10% in a three-week experiment. A slight improvement in copper removal was recorded due to the electric current increasing to 30 mA, indicating that copper removal is not linear with the applied electric current. However, sawdust treatment with HCl lowered the RFM pH, resulting in a total copper removal of 90.30% at electrical currents of 25 mA. Crosslinking sawdust with iron slag by 2% glutaraldehyde achieved a remarkable 97.92% copper removal at 0.18 kWh/kg specific energy from kaolinite soil, while in natural soil, the removal rates for copper, nickel, and zinc reached 26.72%, 54.36%, and 56.44%, respectively after 5 weeks. The discrepancy in heavy metals removal between kaolinite and natural soils reflects the complicated environmental conditions in natural soils on the efficiency of the electrokinetic process when laboratory tests are applied to the field.

F. M. Hamdi · A. Altaee (✉) · Y. Aedan · J. Zhou · M. Mohsen · R. Kardani
Centre for Green Technology, School of Civil and Environmental Engineering, University of Technology Sydney, 15 Broadway, Sydney, NSW 2007, Australia
e-mail: ali.altaee@uts.edu.au

F. M. Hamdi
Department of Civil and Architectural Engineering,
College of Engineering and Computer Sciences, Jazan
University, PO Box 114, 45142 Jazan, Saudi Arabia

M. AL-Ejji · S. J. Zaidi
Center of Advanced Materials, Qatar University, PO
Box 2713, Doha, Qatar

A. H. Hawari
Department of Civil and Environmental Engineering,
College of Engineering, Qatar University, PO Box 2713,
Doha, Qatar

Keywords Electrokinetic · Copper treatment · Soil remediation · Sawdust and iron slag · Reactive Filter Media

1 Introduction

Contaminated soils by various heavy metals are an urgent and prominent global environmental matter,

presenting a substantial threat to the natural ecosystem and human well-being (Ganbat et al., 2023; Hamdi et al., 2024; Wen et al., 2021). Soil samples, for example, were collected from a previous wood impregnation site in the northern region of Copenhagen, Denmark, and exhibited elevated levels of copper, reaching concentrations as high as 1662 mg/kg, along with diverse other heavy metals. Similarly, soil from vineyards in France exhibited copper levels of up to 800 mg/kg (Fagnano et al., 2020; Frick et al., 2019). Consequently, there is an urgent need for remediation technologies that can effectively eliminate heavy metals while minimizing harm to the soil ecosystem (Turan, 2024). One promising approach for remediating soils with low permeability, which are traditionally challenging to clean, is Electrokinetic (EK) treatment. This method entails the application of a low electric current between electrodes inserted into the contaminated soil. Studies (Ghobadi et al., 2021a; Gholizadeh & Hu, 2021; Wen et al., 2021; Yuan et al., 2016) highlighted the effectiveness of EK treatment in addressing soil contamination.

During the electrokinetic (EK) process, heavy metals dissolve in the acidic regions of the soil and accumulate near the cathode. Thus, there is a growing need to improve EK methods by slowing the advance of the alkaline front to facilitate heavy metal removal (Wen et al., 2021). Reducing the pH level promotes the extraction of inorganic contaminants from polluted soils by increasing the release of these metals from the soil's surface (Ganbat et al., 2023; Gholizadeh & Hu, 2021). Enhancement agents are often applied to adjust the catholyte pH and promote acid transport (Fu et al., 2017; Ganbat et al., 2023; Xue et al., 2017; Yu et al., 2019). A study by Bahemmat and co-workers (2016) investigated heavy metal-contaminated soil treatment by catholyte conditioning with 0.1 M HNO₃. Results showed a two to three-fold enhancement in heavy metal remediation efficiency after 3 weeks compared to the unenhanced EK process. Yuan et al. (2016) suggested using CaCl₂ and citric acid to remove inorganic pollutants, reporting better EK remediation results, reduced power consumption, and lowered environmental risks. In a study on chromium waste from industry, Fu et al. (2017) looked at polyaspartic acid and citric acid as two different conditioning electrolytes for EK remediation. The study found citric acid was particularly effective for total chromium removal. Compared to DI water as the electrolyte, citric acid increased

energy due to water electrolysis and heat loss. While strong acids can effectively counteract the alkaline front advancement in soil, they come with trade-offs, including increased energy consumption and the EK treatment period (Fu et al., 2017). Adding conditioning agents can alter specific soil characteristics, including pH levels and conductivity, as observed in the study by Bahemmat et al. (2016). Additionally, it's crucial to consider the electrolyte recovery following EK treatment to manage remediation costs effectively.

To address the limitations associated with conventional EK processes utilizing chemical agents, researchers have explored the use of Reactive Filter Media (RFM) made from materials such as compost, zero-valent iron, activated carbon, and activated bamboo charcoal (Ghobadi et al., 2020, 2021a, 2021b; Xue et al., 2017). These RFMs have demonstrated enhanced performance when compared to traditional EK methods. However, the practical application of these RFMs may need to be improved by cost, availability, and, notably, their life cycle. Consequently, this combined approach to treating EK may need to be more cost-effective (Ganbat et al., 2023; Wen et al., 2021). Recent research has significantly emphasized the development of environmentally sustainable methods to improve EK processes. Research into RFM-enhanced electrokinetics has yielded promising outcomes in various laboratory-scale tests, particularly when employing industrial or agricultural waste materials as the RFM. This approach offers practicality and sustainability by repurposing waste materials (Ganbat et al., 2023; Ghobadi et al., 2021a).

Tests involving RFM-improved EK processes have shown successful application in soils polluted with organic chemicals. For instance, carbonized food waste was utilized in EK processes for copper extraction, showcasing average treatment efficiencies ranging from 53.4% to 84.6% (Han et al., 2010). Compost was also used as an RFM in EK processes for copper removal in a laboratory-scale study, resulting in an impressive removal efficiency of 84.09%. After two cycles of renewal and reuse, the elimination effectiveness remained steady at 74.11% (Ghobadi et al., 2021b). RFMs present numerous advantages in EK processes, such as the adsorption, immobilization, or degradation of contaminants in situ without surface extraction (Cameselle and Reddy, 2012). In this context, investigators have investigated the application of cost-effective, environmentally compatible, and

easy-to-regenerate RFMs, such as compost, biochar, and granular activated carbon, which serve as environmentally sustainable methods to improve the EK process (Ghobadi et al., 2020, 2021b). In another study, soil contaminated with heavy metals from wastewater irrigation of arable lands was treated with charcoal adsorbent from rice stubble (Farhad et al., 2024).

This study utilizes sustainable sawdust (as a cellulose source)/iron slag hybrid RFM to remove copper from kaolinite and heavy metals from contaminated natural soil by the electrokinetic process. Kaolinite was used as a representative model soil to study the effect of experimental factors, without interferences of soil organic and inorganic substances, on the efficiency of the EK before its application to the soil obtained from a contaminated site. Copper was selected as the target contaminant, driven by its widespread presence in contaminated soil (Ghobadi et al., 2020, 2021b). Sawdust and iron slag, waste materials with outstanding adsorption capacity for heavy metals, were mixed to formulate an RFM of desirable physicochemical properties for heavy metals removal by the EK process. Although sawdust's poor conductance to electric current, the excellent electric conductivity of iron slag renders the RFM suitable for the EK application. The elevated alkalinity (pH of 11.38) of the RFM facilitates capturing metal ions but cannot deter the advancement of the alkaline front generated at the cathode. The iron slag/sawdust was crosslinked with glutaraldehyde, and sawdust was functionalized with HCl to enhance the RFM retention capacity to heavy metals and alkaline pH movement in the soil. The study's novelty lies in introducing an environmentally sustainable method of soil treatment by coupling the EK process with a hybrid organic–inorganic sawdust/iron slag RFM. Also, to develop an innovative technique to optimize the electrokinetic process for the removal of copper from kaolinite soil and heavy metal contaminants from natural soil. The research questions are: i) what is the comparative efficiency of removing copper ions from kaolinite with and without the sawdust/iron slag RFM? ii) how does crosslinked glutaraldehyde sawdust/iron slag RFM affect heavy metals adsorption and alkaline front movement in the soil? iii) what are the environmental and soil remediation process implications of implementing the RFM-EK hybrid system? The experiments also explored the impact of electric current intensity and the duration of the EK process on copper extraction from kaolinite soil. The results

of this research will provide insights into the most efficient RFMs for the removal of heavy metals from soil using EKR technology.

2 Materials

2.1 Sample Preparation

The kaolinite soil was sourced from Keane Ceramic Pty, Australia. This soil type was chosen as a standard material for conducting EK tests due to its well-characterized properties. This choice was made due to specific attributes of the soil, namely its minimal organic content, low permeability, and cation exchange capacity. While natural soil samples from the sub-surface at a depth of 15 to 20 cm were obtained from a contaminated site in Sydney (Australia), upon the removal of debris, roots, and stones, the soil was initially air-dried and subsequently sifted through a 600 µm sieve. Table 1 provides detailed information on the characteristics of both the RFM, kaolin soil, and natural soil used in the experiments. The lack of organic matter and the inert nature of the kaolin soil render it exceptionally suitable for investigating the mobility of copper within the EK system under direct electric fields, free from external influences.

Sigma-Aldrich (Australia) provided the copper sulfate (CuSO_4) of 99% purity. Precisely 2.52 g of copper sulfate were dissolved in 1 L of distilled water to create a stock solution containing a concentration of 1000 mg L⁻¹ of Cu^{2+} . This initial stock solution was then diluted to achieve a concentration of 1000 mg L⁻¹, a process repeated for each experiment. The resulting 1L solution was meticulously blended with 1 kg of kaolin soil. Now enriched with copper, the soil was left to stand at laboratory room temperature for at least 72 h (Altaee et al., 2008). Periodic stirring was performed to guarantee a homogeneous distribution of copper across the soil matrix. Finally, the fully saturated soil was carefully packed layer by layer into the EK cell, and uniform compaction was carried out to guarantee an even contaminated soil distribution.

For the RFM, in this study, sawdust was combined with iron slag obtained from an electric arc steel-making furnace at InfraBuild, Australia, and sawdust from a construction project by the Labour Revolution Company, Australia. Electrical conductivity and pH level

Table 1 Characteristics of RFM, Kaolin, and Natural soil

Parameter	kaolin soil	Natural soil	Iron slag	Sawdust/Iron slag	Treated Sawdust/Iron slag	Crosslinked glutaraldehyde sawdust/Iron slag
Particle size analysis (%)						
Less than 1 mm	46.8	13.8	24.89	17.8	17.8	17.8
In between 1 to 2 mm	51.1	65.7	72.5	79.4	79.4	79.4
Greater than 2 mm	2.1	20.5	2.61	2.8	2.8	2.8
Permeability (m/s)	3.95×10^{-10}	1.0×10^{-6}	1.67×10^{-3}	2.35×10^{-2}	2.28×10^{-2}	2.36×10^{-2}
Density (g/cm ³)	1.35	1.42	2.45	1.52	1.51	1.65
TDS (mg/L)	144	303.6	461.5	350.7	348.9	139.4
pH	4.5 ± 0.04	4.76 ± 0.2	11.38 ± 0.04	10.19 ± 0.03	9.24 ± 0.03	9.55 ± 0.05
EC (mS/cm)	0.40 ± 0.05	0.292 ± 0.2	0.643 ± 0.02	0.557 ± 0.02	0.483 ± 0.02	1.478 ± 0.03
Elemental composition (%)						
C	Negligible	5.85	-	-	-	-
O		91.29	-	-	-	-
Fe		2.36	-	-	-	-
Others		1.2	-	-	-	-
Initial metal concentration (mg/kg)						
Cu	1000	216	-	-	-	-
Ni		581	-	-	-	-
Zn		733	-	-	-	-

of the soil were measured using a multimeter model Thermo Scientific (EUTECH PC 450). The readings were acquired by formulating slurries with a dry soil-to-water ratio of 1:5 (weight-to-volume) (Ghobadi et al., 2020). A variety of analytical methods were used to investigate the physical and chemical characteristics of RFMs comprehensively. Data was collected using Energy Dispersive X-ray Spectroscopy (EDX), Zeiss Evo-SEM, and Scanning Electron Microscopy (SEM) techniques. This combination allowed for comprehensive microchemical analysis. Shimadzu Miracle-10 instrument was employed for Fourier Transform Infrared Spectroscopy (FTIR) to examine the RFMs surface functional groups in pre and post-electrokinetic (EK) experiments. The analyses were conducted using a Micrometrics 3Flex surface characterization analyzer operating at 77 K.

2.2 EK Cell Experimental Setup and Design

The experimental arrangement for EK is depicted in Fig. 1. EK experiments utilize a plexiglass reactor with dimensions (cm) of 23 L, 8 D × 11 W. This reactor is designed with two electrode compartments: one for soil and the other for RFM. Inside the soil compartment,

positioned at the boundary between the soil and the cathode chamber, a 1.5 to 2 cm RFM is placed between two filter papers. A perforated plexiglass plate reinforces the filter paper, size 5–13 μm (LLG Labware), acting as a barrier, separating the soil compartment from the electrode chamber to stop soil from infiltrating the electrolyte chambers. A steady electrical current was employed to uphold experimental integrity, facilitated by a direct current power supply, model EA-PS 3015-11B. Hourly measurements and recording of electric current and voltage were carried out by a multimeter (Keithley 175). The reactor's electrode compartments flanking the reactor were equipped with 15 cm × 1 cm (graphite rod electrodes) obtained from Graphite Australia Pty Ltd. Deionized water was employed in both the anolyte and catholyte chambers. To maintain water levels depleted by electroosmotic flow, periodic infusions of ultrapure water were added to the anolyte compartment. The experiment consistently monitored and measured the electroosmotic flow and current intensity. EK tests were conducted at room temperature in the laboratory using constant currents of 20 mA, 25 mA, and 30 mA without controlling the pH level. Table 2 furnishes detailed information on the eight EK experiments. Milli-Q water served as the

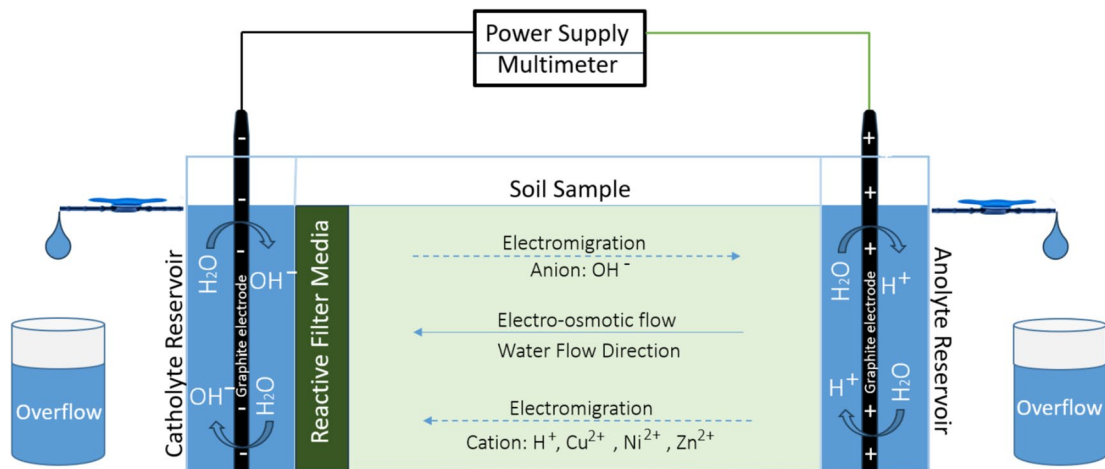


Fig. 1 Schematic illustration of metal treatment by EK-RFM hybrid system

anolyte, and the solution level in the inflow reservoir was meticulously controlled to sustain a consistent level, ensuring a constant hydraulic gradient across the soil sample. The EK experiments persisted for durations spanning two to three weeks.

To assess the efficacy of the enhanced RFM-EK test, Exp1 served as a baseline experiment, focusing on Cu removal from kaolin soil without an RFM at 20 mA steady currents. Exp2 delved into the effect of a standalone iron slag RFM at 20 mA electric currents

for copper extraction from the contaminated soil. Exp3 investigated the impact of a mixture of sawdust/iron slag-RFM at 20 mA current intensity. Exp4 and Exp5 studied the impact of raising the electric current from 20 to 30 mA on the efficiency of the sawdust/iron slag RFM-EK system for copper treatment. Exp6 scrutinized the influence of treating sawdust with HCl to lower its pH in the sawdust/iron slag RFM-EK system at 25 mA electric currents for copper treatment. Exp7 studied glutaraldehyde (Sigma-Aldrich,

Table 2 Description of the EK-RFM system

Experiment	Type of soil	RFM type	Metals	Metal (mg/kg)	RFM	Current (mA)	Period (day)
Exp1	Kaolin Soil	EK only	Cu	1000	NA	20	14
Exp2	Kaolin Soil	EK- Iron slag	Cu	1000	100% Iron slag	20	14
Exp3	Kaolin Soil	EK- SD/Iron slag	Cu	1000	50% Sawdust + 50% Iron slag	20	21
Exp4	Kaolin Soil	EK- SD/Iron slag	Cu	1000	50% Sawdust + 50% Iron slag	25	21
Exp5	Kaolin Soil	EK- SD/Iron slag	Cu	1000	50% Sawdust + 50% Iron slag	30	21
Exp6	Kaolin Soil	EK- TSD/Iron slag	Cu	1000	50% Treated Sawdust + 50% Iron slag	25	21
Exp7	Kaolin Soil	EK- SD/Iron slag + GA	Cu	1000	50% Sawdust + 50% Iron slag and 2% glutaraldehyde	25	21
Exp8	Natural Soil	EK- SD/Iron slag + GA	Cu, Ni, and Zn	216,581, and 733	50% Sawdust + 50% Iron slag and 2% glutaraldehyde	25	35

Australia) crosslinking with sawdust in the RFM. A 2% glutaraldehyde was mixed with sawdust and iron slag to ensure homogeneity of the RFM in the EK process operating at a 25 mA electric current. The concentration of glutaraldehyde was 2% i) to reduce the environmental toxicity of glutaraldehyde, ii) to maintain a desirable biodegradability of glutaraldehyde compounds in soil, iii) over-crosslinking will reduce the RFM flexibility and surface area, block active functional groups, and change the surface charge of the crosslinked RFM. Finally, Exp8 utilized an RFM-EK process with sawdust/iron slag and 2% glutaraldehyde, conducted over 35 days for Cu^{2+} , Ni^{2+} , and Zn^{2+} mixture removal from a contaminated site. EK optimization considered the following critical operating factors: RFM use, electrical current, sawdust pH adjustment, and EK operating time.

2.3 RFM Adsorption/Desorption Tests

The adsorption performance of the composite material, composed of sawdust and iron slag, was evaluated utilizing a temperature-controlled shaker operating under a precise environment at 24 ± 1 °C. The shaker operated at a constant rotational speed of 150 revolutions per minute (rpm) throughout the assessment, which extended from 4 to 24 h. The concentrations of solid-to-liquid ratios for copper sulfate and the composite solution were standardized at 2.52 g/L. The adsorption capabilities of the composite adsorbent (a blend of sawdust and iron slag in a 1:1 proportion) were investigated for their affinity towards copper. Post adsorption, the composite material (sawdust/iron slag) was separated via centrifugation at 10,000 rpm for 15 min. The levels of copper in the isolated samples were determined through analysis using Inductively Coupled Plasma Mass Spectrometry (ICP-MS). The capacity of adsorption, expressed in milligrams per gram (mg/g), was determined utilizing Eq. (1).

Capacity of adsorption

$$q_e \left(\frac{\text{mg}}{\text{g}} \right) = \frac{(C_i - C_r) * V}{W} \quad (1)$$

The formula for adsorption capacity takes into account C_{initial} (mg L⁻¹) as the initial Cu^{2+} concentration, C_{residual} (mg L⁻¹) is the equilibrium Cu concentration, V (liters) is the volume of the solution,

and W (grams) is the weight of sawdust/iron slag. The assessment of copper adsorption onto the sawdust/iron slag involves the construction of elution curves utilizing the C_f/C_i ratio. In this context, C_i denotes the initial concentration of pollutants, while C_f represents contaminants concentration at a specific period, t . Breakthrough curve tests are crucial for identifying the point of breakthrough, which indicates the effluent concentration reaching a specified percentage of the influent concentration (Rahchamani et al., 2011).

Following the completion of the adsorption test, desorption experiments were carried out to evaluate the reversibility of the process and measure the copper released from adsorption. In vials, sawdust mixture and iron slag were subjected to a 0.1 M hydrochloric acid (HCl) solution (50 mL). Desorption was also conducted on a temperature-controlled shaker at 24 °C and 150 rpm for 24 h. After desorption, the solution was separated from the sawdust/iron slag mixture by centrifugation at ten thousand rpm for fifteen minutes to isolate the components effectively. Inductively coupled plasma (ICP) measured the copper concentrations in the RFM specimen. Desorption capacity (expressed in mg per g) and measured by Eq. (2).

$$\text{Desorption} \left(\frac{\text{mg}}{\text{g}} \right) = \frac{(C_r) * V}{W} \quad (2)$$

C_{residual} (mg per litre) represents the equilibrium residual concentration of Cu, W (g) stands for sawdust/iron slag weight, and V (L) is the solution volume.

Utilizing adsorbents over multiple cycles demonstrates clear cost-saving benefits by reducing expenses related to the adsorption process, making them highly valuable for various industrial uses. The adsorbents' reusability was assessed through adsorption-desorption experiments within a singular cycle. Desorption assessments were conducted under acidic conditions of pH 1.4, and employing Eq. (3) to calculate the desorption (D).

$$D(\%) = \left(\frac{C_{\text{desorbed}}}{C_{\text{adsorbed}}} \right) * 100 \quad (3)$$

In Eq. (3), the desorbed Cu ions are represented by C_{desorbed} , and C_{adsorbed} represents the adsorbed Cu ions.

2.4 Analytical Methods

After completing the EK tests, the soil was partitioned into six equal segments labeled Sect. 1 (S1) through Sect. 6 (S6). Each segment was thoroughly mixed and dried in the oven for 12 h at 100 °C. Afterward, the soil segments were analyzed for Cu^{2+} concentrations in Exp1 to Exp7 (kaolin soil) and for Cu^{2+} , Ni^{2+} , and Zn^{2+} ion concentrations in Exp8 (natural soil). A soil suspension was prepared by mixing dry soil with DI water in a 1:5 ratio (weight/volume). The mixture was agitated for more than 5 min prior to utilizing a (HACH HQ40 d model) multimeter for pH levels and electric conductivity (EC) measurements of the soil. ICP-MS was employed to determine copper concentration. Following the drying and homogenization of the soil sections, two samples were taken from each section. Every sample was subjected to a digestion procedure involving 2 M of HNO_3 (nitric acid), adding 10 ml of HNO_3 /g dry soil, following the methodology detailed. The mixture of soil acid was shaken at 250 rpm for four hours. Subsequently, soil suspension underwent centrifugation (Three thousand rpm for three minutes) to facilitate the separation of the solution from soil particles (Groenenberg et al., 2017). The RFM was extracted in a manner similar to the soil samples and subsequently analyzed for copper concentration. Equations (4) and (5) were utilized to assess copper removal efficiency and determine specific energy consumption (SEC) during the electrokinetic process, respectively (ref).

$$\text{Removal efficiency} = \frac{C_i - C_f}{C_i} 100\% \quad (4)$$

$$E_u = \frac{10^{-3}}{V_s} \int_0^t V I dt \quad (5)$$

C_i (mg/kg) represents the Cu^{2+} preliminary concentration, and C_f (mg/kg) denotes the remaining Cu^{2+} concentration following EK tests. E_u (measured in kWh kg^{-1}) stands for the specific power consumption, V (measured in V) represents the applied voltage, and I (measured in A) indicates the electric current. The experimental period is denoted by t (measured in hours), and V_s (measured in kg) signifies the total mass of the treated soil.

3 Results and Discussion

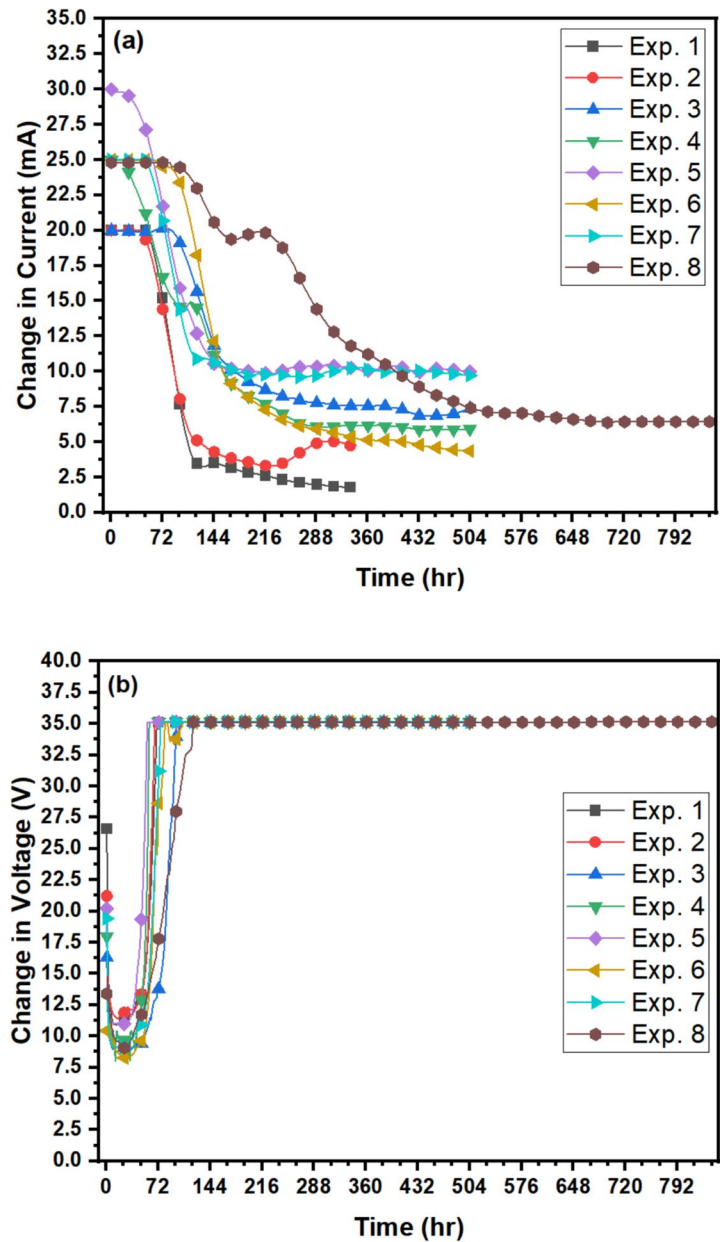
3.1 The Electric Current

During water electrolysis, hydronium ions (H_3O^+) are generated at the anode, while hydroxide ions (OH^-) are produced at the cathode electrode. Consequently, an acid and alkaline front emerges, migrating toward their respective electrodes within the soil (Hamdi et al., 2024; Hawal et al., 2023). Acid front transport through the soil solubilizes metal ions and carries them toward the cathode. Figure 2 illustrates soil voltage and electric current variations across different EK tests. A clear connection exists between the electric current and the quantity of electric charge moving through the soil pores, exhibiting an inverse relationship with the transfer of electrons (Hamdi et al., 2024; Hawal et al., 2023).

At the onset of different EK experiments, the initial electric currents were approximately 20 mA, 25 mA, and 30 mA (Table 2) and gradually declined after 48 to 96 h. The correlation between the electric current in the soil's EK cell and the concentration of free ions underscores the significant impact of electric current on the movement of contaminants through the soil. The initial stability in electric current for several hours can be attributed to the occurring anode electrolysis reaction and the subsequent increase in dissolved ions within the solution pores. Nevertheless, an overtime decrease in electric current results from the merging of acid and alkaline fronts and the buildup of charged molecules within the soil sample. The reduction in charged particles in the soil led to a decrease in the electric current. Therefore, the presence of charged soil particles decreased, reducing the electric current (Ganbat et al., 2022, 2023; Hamdi et al., 2024; Hawal et al., 2023).

Figure 2a depicts a noticeable decline in electric current between 48 and 96 h across Experiments 1–8. The most pronounced drop was observed in Exp1, conducted without RFM, facilitating alkaline front progression near the cathode zone within the soil. A similar trend was observed in Experiment 2, where all iron slag RFM was used. In this instance, after 72 h of operation, the electrical current decreased from an initial 20 mA to 17 mA and further dropped to 3.10 mA after 240 h. Subsequently, an unexpected increase occurred, rising to 4.20 mA after 264 h and eventually reaching 4.80 mA by the end of the

Fig. 2 (a) Electric current variation during EK tests at 20, 25, and 30 mA. (b) Corresponding voltage changes, showing the influence of current and soil interactions on EK efficiency



experiment, possibly attributed to the dissolution of ionic components due to the advancing acid front in the later stages of the EK test. Exp3 aimed to mitigate the progression of the alkaline front by utilizing a mixture of 50% sawdust (SD) and 50% iron slag, coupled with an extension of the EK duration to three weeks. During Experiment 3, which extended over three weeks and involved mixing iron slag with sawdust, the electric current held steady at 20 mA for 96 h. The lower pH of SD-iron slag RMF in

Experiment Exp3 than in Exp2 suppressed the alkaline from movement in the soil and maintained the electric current for a longer time. Subsequently, electric current experienced a gradual decrease, dropping to 7.5 mA by the third week attributed to metal hydroxide precipitation and the interaction between alkaline and acid fronts in the soil.

Exp4 replicated the operating conditions of Exp3, with an increase in the electrical current to 25 mA to facilitate the acid front transport through the

Kaolin soil. The electric current experienced a significant decline from 25 mA to 20.2 mA after 48 h due to the precipitation of metal hydroxides and the convergence of the acid and alkaline fronts within the soil. Following this, it continued to decrease to 17.1 mA after 72 h and ultimately reached 6 mA by the conclusion of the experiment. During Experiment 5, when the EK electric current was raised to 30 mA, it initially held at 29.49 mA for 24 h, gradually decreased to 12.6 mA after 120 h, and subsequently fluctuated between 9.10 and 11 mA. Exp6 was conducted at an electric current of 25 mA, treating sawdust with HCl to lower the pH of the RFM, aiming to mitigate the progression of the alkaline front in the soil. The maximum electric current reached 24.26 mA, slightly lower than that observed in Experiment 4. This reduction can be attributed to the reduced EC of the RFM used in Exp6 (Table 1). Notably, there was a significant decline in the electric current, dropping from 24.26 mA to 15 mA after 96 h. This decline likely resulted from the precipitation of metal hydroxides and the convergence of the acid and alkaline fronts. By the conclusion of Exp6, the electric current had decreased even further to 4.5 mA. Exp7 was conducted at 25 mA, using an RFM composed of a 50% sawdust (SD) and 50% iron slag mixture. The mixture was treated with a 2% glutaraldehyde to enhance its adsorption properties. The primary objective of this experiment was to mitigate the progression of the alkaline front in the soil, which is a common challenge in electrokinetic treatments. The use of glutaraldehyde aimed to improve the structural integrity and reactivity of the RFM, enhancing its ability to capture and immobilize metal ions while controlling the pH changes in the soil section near the cathode. The electric current remained constant at 23 mA for 72 h, then gradually decreased and stabilized at around 10 mA until the end of the experiment. In Exp8, conditions from Exp7 were replicated with a key modification that the duration was extended to 5 weeks, and natural soil replaced kaolinite to evaluate the effectiveness of the EK process in removing Cu^{2+} , Ni^{2+} , and Zn^{2+} ions from a contaminated site. The electric current initially dropped from 25 mA to 19.35 mA after 168 h, then fluctuated slightly before declining again due to metal hydroxide precipitation and the convergence of acid and alkaline fronts in the soil. By the experiment's end, the current had decreased further to 6.45 mA.

As illustrated in Fig. 2b, there is a discernible adverse correlation between the electric current and

the voltage change. The precipitation of metal ions decreased the electric current while simultaneously leading to an increase in voltage, which can be attributed to the heightened soil resistivity. Across all EK tests, a consistent trend was observed wherein the voltage declined initially within the initial 24-h period. This decline was probably attributed to the solubilization of metal ions and a subsequent rise in the concentration of ions within the soil's pore fluid. Initial voltage readings ranged from 10.44 to 20.5 V, declining to approximately 9 V after 24 h.

Interestingly, a subsequent voltage surge to nearly 35.12 V was observed in Experiments 1, 2, 4, and 5 after 48 h and in Experiments 3, 6, 7, and 8 after 120 h. This increase was attributed to the greater soil conductivity and ionic strength observed in Experiments 3, 6, 7, and 8. Compared to standard processes, EK experiments involving RFM exhibited higher electric currents since the alkaline front movement was slowed down, preventing early metal ions precipitation in the soil.

3.2 Electric Conductivity and pH

Figure 3a illustrates the pH distribution across soil sections S1 through S6, ranging from the anode to the cathode, after the EK tests. It is essential to highlight that the EK tests were conducted without controlling the pH. By the conclusion of the EK treatment, the pH of the soil in regions proximal to the anode compartment decreased below the initial pH, subsequently increasing gradually towards the cathode zone. At the anode, soil sections S1 to S3 displayed acidity due to the advancement of the acid front resulting from electrolysis, leading to the generation of H^+ ions. This phenomenon is influenced by the higher ionic mobility of hydrogen ions, which move approximately 1.8 times faster than hydroxide ions (Ganbat et al., 2023; Ghobadi et al., 2021b).

Figure 3a represents pH differences in the soil sections Exp1 and RFM-enhanced Exp2 to Exp8. In Exp1, soil sections S1 to S5 consistently maintained acidic pH levels. In contrast, section S6, close to the cathode, recorded a pH of 6.5 due to the rapid migration of OH^- ions. On the contrary, in RFM-enhanced Exp2, a discernible pH increase is observed from the soil section S1 toward the RFM. The high pH of the RFM is due to its initial alkalinity of 11.38 (Table 1), which negatively affected the transport of H^+ ions close to

the cathode. Interestingly, the pH in the cathode tank remains stable at pH 12.71, while the pH of sections S4 to S6 adjacent to the cathode fluctuates. Specifically, in Exp2, the pH across soil sections S1 to S5 increased from 2.20 to 4.08. In contrast, the alkaline nature of the RFM facilitated the rapid migration of OH^- ions in the soil, resulting in section S6 reaching a pH of 7.04.

However, the incorporation of 50% sawdust into the iron slag RFM acted as a buffer, impeding the movement of alkaline pH toward the anode. Sawdust contains cellulose that interacts with hydroxyl ions in an alkaline solution, potentially reducing pH through absorption. The cellulose hydroxyl groups have an affinity to the hydroxyl generated at the cathode, slowing down alkaline front movement in the soil. As a result, the acid front progressed faster towards

the cathode in Exp3 compared to Exp2. In Exp3, pH levels ranged from 3.00 to 4.06 across soil sections S1 to S5, while section S6 reached a pH of 5.43. The lower pH of section S6 in Exp3 is attributed to the RFM pH of 10.19 compared to the RFM pH of 11.38 in Exp2. The lower RFM pH in Exp3 hindered the rapid movement of the alkaline front in the soil, thereby enabling the propagation of the acid front in soil section S6. In Exp4, the electrical current was increased to 25 mA. It was observed that there was a decrease in soil pH of sections S1 and S2, reaching pH 2.6, while for sections S3 to S6, the pH ranged between 3.15 and 4.60. Notably, the RFM's pH was 9.63, which decreased from the initial pH of 10.19. The decline in soil pH likely resulted from increased electrical currents, facilitating the movement of acidic

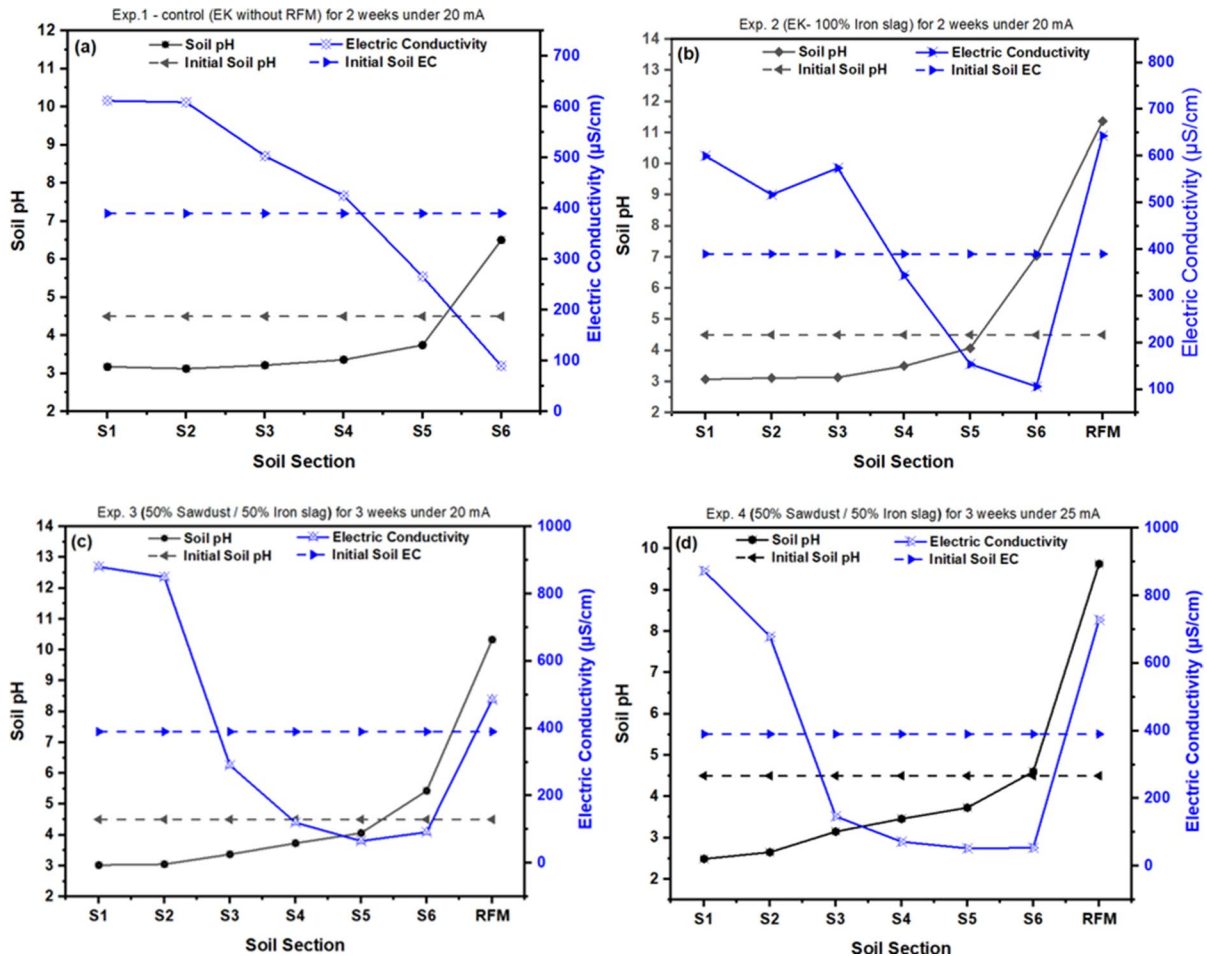


Fig. 3 pH and EC of the soil post-remediation across the sections from the anode to the cathode (a) Exp1 (control) (b) Exp2 (c) Exp3 (d) Exp4 (e) Exp5 (f) Exp6 (g) Exp7 (h) Exp8

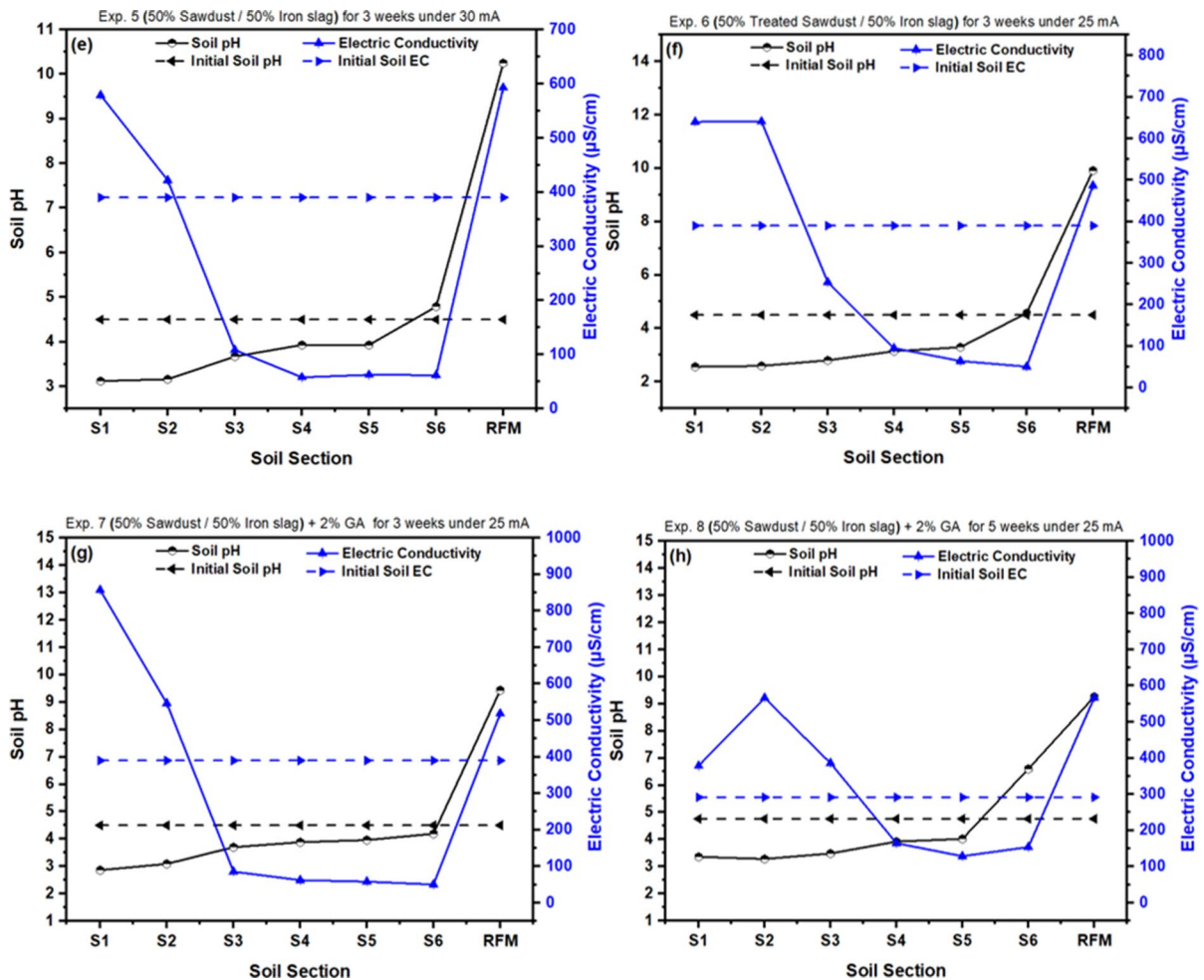


Fig. 3 (continued)

components toward the cathode zone. However, raising the electric current to 30 mA in Exp5 slightly increased sections S1 and S2 pH to 3.15 compared to pH 2.6 in Exp4. For sections S3 to S6, the pH ranged between 3.70 and 4.80. Also, the pH of the RFM was 10.25 at the end of the test. In Exp6, the sawdust was treated with HCl to lower its pH from 8.11 to 5 before mixing with iron slag to reduce the RFM pH to 9.24 (Table 1). Sections S1 to S5 recorded pH values lower than the initial pH, ranging from 2.50 to 3.30, while section S6 showed a slightly higher pH than the initial value, measuring pH 4.57.

Nevertheless, the integration of 50% sawdust with 50% iron slag RFM and 2% Glutaraldehyde in Exp7 facilitated slowing down the advancement of the alkaline pH toward the anode. All sections from

S1 to S6 exhibited pH levels lower than the initial value, ranging between 2.80 and 4.10. Compared to other experiments, Exp7 demonstrated the lowest range of pH level in S1-S6 because of the initial RFM low pH of 9.55, deterring alkaline front rapid movement in the soil and enabling the mobility of H^+ ions toward the cathode. Notably, the elevated pH levels in soil sections adjacent to the cathode result in a negative soil surface charge, thereby enhancing the adsorption of Cu^{2+} through increased electrostatic interaction with the positively charged Cu^{2+} ions (Ghobadi et al., 2021b). In Exp8, the sawdust/iron slag was crosslinked with 2% Glutaraldehyde to effectively slow down the advancement of the alkaline pH toward the anode and reduce the RFM pH to 9.55 (Table 1). Sections S1 to S5 recorded pH values

lower than the initial pH, ranging from 3.36 to 4.02, while section S6 showed a higher pH than the initial value, measuring pH 6.60.

As depicted in Fig. 3a, in Exp1 without RFM, soil pH in sections (S1-S5) was acidic (ranging from pH 3.18 to pH 3.75) and increased toward the cathode, reaching pH 6.5 in section S6. In Exp2 (Fig. 3b), the pHs of sections (S1-S5), from 2.20 to 4.08, were lower than the initial soil pH and increased to 7.04 in S6. The elevated pH level in the cathode zone of Exp2 is likely due to the higher iron slag content in the RFM. In Fig. 3c, Exp3 displayed soil pH from 3.00 to 4.06 in sections (S1 to S5), increasing to pH 5.43 in section S6. The decrease in pH of soil S6 was likely due to the lower pH of the sawdust/iron slag RFM (10.19), contributing to the acid front advancement in the soil. In Exp4 (Fig. 3d), sections (S1 to S5) recorded pH values from pH 2.49 to 3.73, slightly increasing to 4.60 in soil section S6 near the cathode. Figure 3e illustrates that in Exp5, the pH in sections (S1 to S5) ranged from pH 3.12 to 3.93, significantly increasing to pH 4.80 in section S6. Exp6 (Fig. 3f) exhibited a low pH of 2.56 to 2.80 in soil sections S1 to S3, increasing to pH 3.14 and 3.29 in sections S4 and S5 and further increasing to pH 4.57 in section S6. Exp 7 (Fig. 3g), the pH levels across sections (S1 to S6) were consistently low, ranging from 2.80 to 4.10, which was lower than the initial pH. In Exp8 (Fig. 3h), the pH across sections S1 to S5 remained consistently low, ranging from 3.36 to 4.02, below the initial pH of 4.76 (Table 1), while section S6 pH was 6.60.

Prior studies corroborate these results, suggesting an inverse relationship between soil pH and soil electrical conductivity (EC) (Ghobadi et al., 2021a, 2021b; Hamdi et al., 2024). The EC of soil is pivotal in the electrokinetic (EK) process, facilitating the migration of pollutants and charged particles in response to direct electric current. Throughout the EK process, the migration of charged particles towards the positive and negative electrodes establishes a gradient in concentration, influencing soil resistivity and pH modification. When the soil has high electrical conductivity (EC), it can conduct electrical charges. However, the removal of ionic species during EK treatment can lead to a decrease in EC. In this study, an SD-iron slag, strategically placed near the cathode to capture metal ions and prevent the advancement of an alkaline front, exhibited slightly

higher conductivity than the kaolinite soil (Table 1). Figure 3 indicates a lower EC in soil with low ion concentrations. Soil's EC exhibited a consistent decrease from the anode to the cathode zone across Exp1 to Exp8, indicating a higher concentration of free ions near the anode. Generally, using RFM with acid-treated sawdust mixed with iron slag assisted in maintaining the soil pH below the initial levels in all sections and prevented the advancement of the alkaline front in the soil (Fig. 3f). The EC of soil S1-S3 in all EK experiments increased, resulting from the increase of ionic species, notably associated with free protons. Across all experiments, a decline in EC was observed in soil S4-S6, attributed to the convergence of acid and alkaline fronts close to the cathode zone.

3.3 Removal of Contaminant

Figure 4a shows the distribution of Cu^{2+} across kaolinite soil sections and the RFM, while Fig. 4b presents the distribution of Cu^{2+} , Ni^{2+} , and Zn^{2+} ions across natural soil sections and the RFM at the end of the EK process. The positively charged Cu^{2+} , Ni^{2+} , and Zn^{2+} ions dissolved and migrated toward the cathode. In the Ek tests without RFM, significant deposition of Cu^{2+} occurred near the cathode due to the alkaline pH, leading to the precipitation of metal hydroxides (Ghobadi et al., 2021a, 2021b; Hamdi et al., 2024; Hawal et al., 2023). Based on these results, iron slag and sawdust/iron slag RFMs were employed to capture metal ions in experiments Exp2 to Exp8. Figures 4a&4b show a substantial Cu^{2+} , Ni^{2+} , and Zn^{2+} migration and accumulation near the soil Sect. 6 and in the RFM.

Exp1 to Exp7 were conducted to extract Cu^{2+} ions from the polluted kaolinite soil, and Exp8 was conducted to extract Cu^{2+} , Ni^{2+} , and Zn^{2+} ions from a contaminated site (Table 2). In Exp1 to Exp3, an electric current was 20 mA, while Exp4, Exp6, Exp7, and Exp8 employed 25 mA, and Exp5 used 30 mA to study the impact of increasing electric current and RFM on EK performance. Exp1 and Exp2 had a duration of 2 weeks, whereas Exp3 to Exp7 were carried out over 3 weeks, and Exp8 was 5 weeks with natural soil. In Exp1, copper concentration was nearly eliminated from section S1, gradually increasing across sections S2-5 and spiking to 3486 mg. L⁻¹ in section S6 (Fig. 4a). Nevertheless, the total depletion of copper from the soil amounted to approximately 3.21%

Fig. 4 (a&b) Residual metal concentration in soil sections/RFM after EK, and (c) Total metal removal/ Specific Energy Consumption at the end of the EK

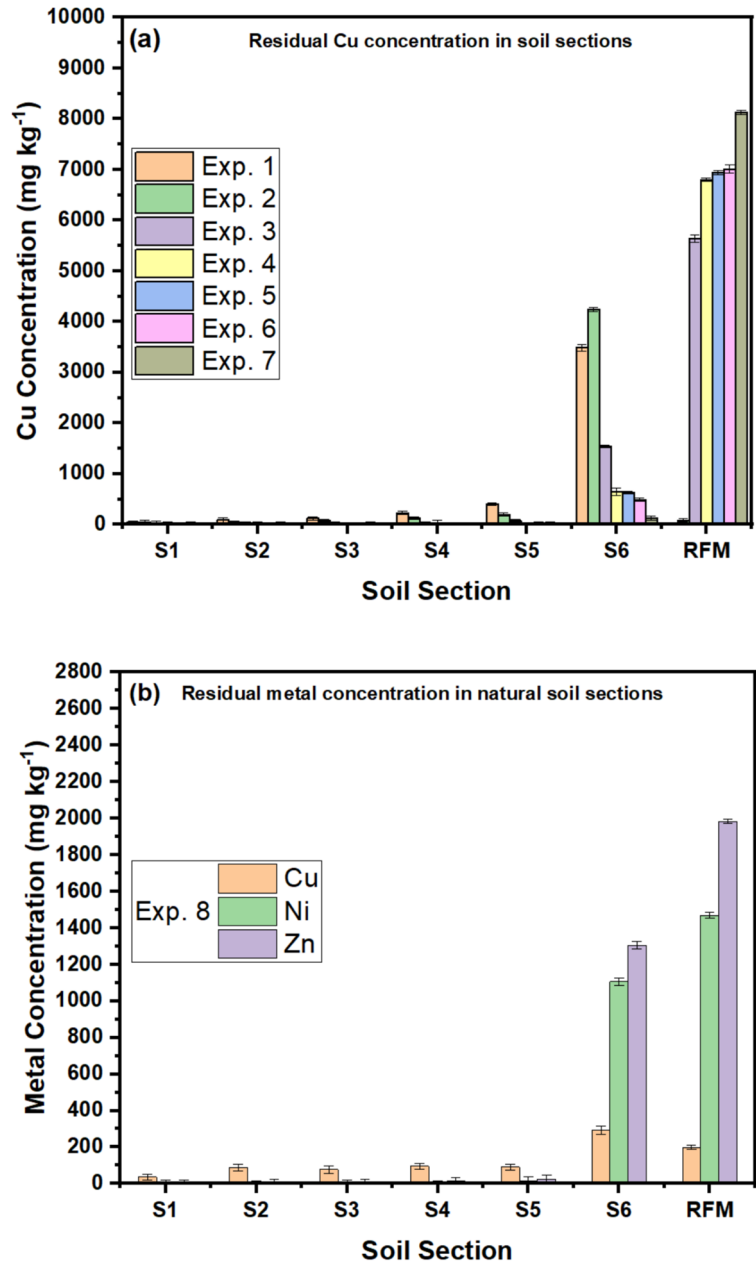
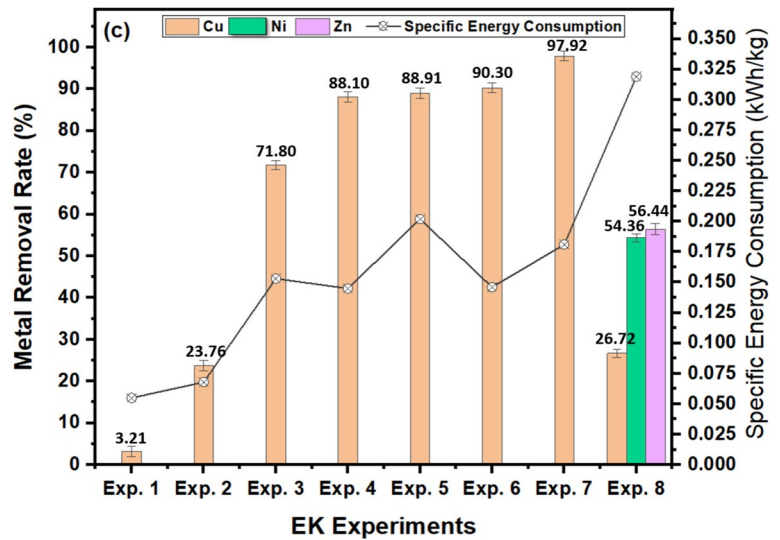


(Fig. 4c). In Exp2, iron slag RFM closed to the cathode notably boosted the removal of Cu^{2+} throughout soil sections S1 to S5. A considerable amount of copper precipitated in section S6, which is attributed to the alkaline pH of the soil. The concentration of Copper ranged from 44 mg. L^{-1} in S1 to 4242 mg. L^{-1} in S6. The alkaline conditions in S6 promoted the precipitation and adsorption of copper onto the soil surface. The correlation between soil pH and Cu^{2+} adsorption

confirms that Cu^{2+} adsorption is pH-dependent (Ghobadi et al., 2021b; Hamdi et al., 2024). When pH levels fall below the point of zero charge (pH_{zpc}), the soil exhibits a positive charge, which shifts to a negative charge as the pH surpasses the pH_{zpc}. Cu^{2+} adsorption intensifies when the soil exhibits a negative charge near the cathode region, characterized by a pH higher than the pH_{zpc} of 4.5. Conversely, Cu adsorption diminishes in the vicinity of the cathode area due to

Fig. 4 (continued)



the elevated soil pH, exceeding the pH_{zpc} of 4.5. Only 216.4 mg. L^{-1} of copper concentration was detected in the iron slag RFM. Iron oxide, the predominant component of iron slag, demonstrates a strong affinity for adsorbing heavy metals (Yeongkyoo, 2018). Iron oxide retains heavy metals through mechanisms such as surface complexation, electrostatic interactions, and precipitation (Hu et al., 2018). While achieving a higher rate of removing copper (seven times higher than Exp1), Exp2 still exhibited a relatively low removal efficiency, capturing approximately 21.76% of the Cu^{2+} in the RFM (Table 3). Moreover, the alkaline pH of RFM promoted the movement and propagation of OH^- ions from the cathode to the anode. Exp3 utilized sawdust with iron slag to reduce the RFM pH from 11.38 to 10.19, slowing the rapid movement of the alkaline front from the cathode (Table 1). Sawdust also releases acidic components when exposed to hydroxyl ions. Its alkaline nature helps neutralize excess hydroxyl ions, maintaining a stable pH environment. Exp3 achieved a notable removal improvement of copper across the majority of soil sections, with 67.66% of the copper accumulating in the RFM and achieving an overall removal rate of 71.8% (Table 3). The concentration of copper decreased from 21.5 mg. L^{-1} in soil S1 to $1539.5 \text{ mg. L}^{-1}$ in S6, achieving $5638.5 \text{ mg. L}^{-1}$ in the RFM (Fig. 4a). The predominant acidic conditions observed in the majority of soil sections during Exp3 significantly improved the extraction of copper compared to Exp2.

The electric current was increased in Exp4 to Exp8 to enhance the electrolysis reaction and copper, nickel and zinc removal from the soil. As depicted in Figs. 4a&4b, copper was extracted from soil S1-6 and gathered in the RFM during Exp4. Copper concentration in S1 was 16 mg. L^{-1} and increased incrementally in subsequent sections, peaking at 646.5 mg. L^{-1} in S6 and reaching $6801.5 \text{ mg. L}^{-1}$ in the RFM. Approximately 82.22% of the copper was retained in the RFM (Table 3), resulting in an overall copper removal rate of 88.10% for Exp4. The improved extraction of copper noted in Exp4, compared to Exp3, was attributed to the rise in electric current from 20 to 25 mA. This increase effectively bolstered the progression of the acid front within the soil. Consequently, the acid front propagated through the soil, solubilizing and transporting the copper ions towards the RFM. Increasing the electrical current from 25 to 30 mA in Exp5 did not lead to a significant improvement in copper concentration (Fig. 4a). The copper concentration for sections S1 to S6 was slightly less than that for the soil sections in Exp 4, and it reached 6939 mg. L^{-1} in S6. The RFM accumulated 83.27% of the copper, resulting in a total copper removal of 88.91% by the end of Exp5 (Table 3), approximately 1% higher than in Exp4. EK experiments show that increasing the electric current from 25 to 30 mA led to only a slight improvement in copper removal (< 1%) from 88.10% to 88.91%, highlighting a non-linear relationship between current intensity and EK efficiency. While higher currents can boost ion migration

Table 3 Removal efficiency and Mass Balance of EK experiments

Exp No	Type of soil	Metal ions	Initial Metal in soil (mg)	Residual Metal in Soil (mg)	Metal in RFM (mg)	Electrolyte/pore water Metal (mg)	Mass Balance (%)	Total metal removal (%)
Exp1	Kaolin Soil	Cu	1000	968.19	N/A	1.5	102.17	3.21 ± 0.31
Exp2	Kaolin Soil	Cu	1000	761.94	216.4	0	101.72	23.76 ± 0.38
Exp3	Kaolin Soil	Cu	1000	281.50	676.62	4.5	101.15	71.80 ± 0.19
Exp4	Kaolin Soil	Cu	1000	118.58	822.18	4.5	102.50	88.10 ± 0.30
Exp5	Kaolin Soil	Cu	1000	111.00	832.68	1	101.88	88.91 ± 0.24
Exp6	Kaolin Soil	Cu	1000	97.25	841.38	1.5	102.48	90.30 ± 0.20
Exp7	Kaolin Soil	Cu	1000	20.82	976.02	0.5	100.29	97.92 ± 0.23
Exp8	Natural Soil	Cu	216	158.29	209.69	0.2	103.30	26.72 ± 0.26
		Ni	581	265.14	505.85	0.1	101.92	54.36 ± 0.25
		Zn	733	319.27	514.41	0.1	100.80	56.44 ± 0.29

and electroosmotic flow, they also intensify water electrolysis, creating sharp pH gradients that may cause Cu^{2+} precipitation or immobilization before reaching the RFM. Additionally, increased current raises energy consumption and costs without proportional gains in performance. Issues like electrode polarization and overheating may also arise. The results suggest that a 25 mA electric current is more effective for running the EK-RFM system, while a higher electric current offers no benefit. Thus, careful current optimization is crucial to balance efficiency, energy use, and system stability. Therefore, Exp6 was conducted at 25 mA electric current, with sawdust treated with HCl to lower the pH of the RFM, aimed at buffering the advancement of the alkaline front. The concentration of Cu^{2+} in (S1) was 15.5 mg. L⁻¹ and increased to 490 mg. L⁻¹ in S6 while reaching 7011.5 mg. L⁻¹ in the RFM, as shown in Fig. 4a. The RFM accumulated 84.14% of the copper, resulting in a total copper removal of 90.30% at the end of the 3-week EK process (Fig. 4c). In addition, the introduction of glutaraldehyde to sawdust/iron slag RFM in Exp7 significantly improved the efficiency of Cu^{2+} removal. Glutaraldehyde created a homogenized and reactive composite material, enhancing the adsorption capacity of the sawdust/iron slag RFM (Figure A1c), leading to more effective immobilization of Cu^{2+} , thereby increasing the overall efficiency of the EK process compared to experiments Exp1 to Exp6. Introducing glutaraldehyde in Exp7 modified the surface property of RFM by increasing surface polarity

and enhancing interactions with OH^- ions through hydrogen bonding or electrostatic attraction. Thus impeding alkaline front migration toward the anode and maintaining a lower pH throughout the experiment. This reduction in pH was responsible for enhancing the removal of Cu^{2+} , creating an acidic environment conducive to the dissolution and migration of metal ions, and ultimately improving the efficiency of the EK process. The concentration of copper in S1 was 0.155 mg. L⁻¹ and increased to 123.5 mg. L⁻¹ in S6 while reaching 8133.5 mg. L⁻¹ in the RFM (Fig. 4a). The RFM captured 97.60% of the Cu^{2+} , resulting in 97.92% removal (Table 3).

Exp8 evaluated the effectiveness of the EK combined with sawdust with iron slag RFM and glutaraldehyde for Cu^{2+} , Ni^{2+} , and Zn^{2+} ions removal from contaminated soil. The concentrations of Cu^{2+} , Ni^{2+} , and Zn^{2+} were 216, 581, and 733 mg. L⁻¹, respectively (Table 1). The concentration of Cu^{2+} in soil sections S1 to S6 ranged from 35.5 to 291.5 mg. L⁻¹, while Ni^{2+} and Zn^{2+} concentrations were lower than Cu^{2+} . Ni^{2+} concentrations ranged from 4.75 mg. L⁻¹ in S1 to 1107.5 mg. L⁻¹ in S6 and Zn^{2+} concentrations ranged from 5.5 mg. L⁻¹ in S1 to 1305 mg. L⁻¹ in S6. The concentrations of Cu^{2+} , Ni^{2+} , and Zn^{2+} in the RFM were measured at 199, 1469.5, and 1984.5 mg. L⁻¹. The RFM was effective in capturing 21.03% of Cu^{2+} , 50.58% of Ni^{2+} , and 54.14% of Zn^{2+} (Table 3), achieving 26.72%,

54.36%, and 56.44% removal for Cu^{2+} , Ni^{2+} , and Zn^{2+} by the end of the EK process (Fig. 4c).

The application of sawdust-iron slag RFM significantly enhanced copper removal across Experiments 3 to 7. Initially, copper removal was 3.21% in Exp1, increasing to 23.76% in Exp2 with the introduction of iron slag RFM. Exp3 demonstrated further improvement in copper removal by combining sawdust with iron slag, leveraging sawdust's affinity for alkaline pH. In Exp4, increasing the electric current to 25 mA achieved 88.10% removal. Exp5 showed marginal enhancement in copper elimination with an electric current of 30 mA, indicating non-linear effects that should be optimized during the EK process. Exp6, where sawdust was treated with HCl to lower RFM pH, achieved a total copper removal of 90.30%. Exp7, the integration of sawdust with iron slag RFM and glutaraldehyde effectively slowed down the advancement of the alkaline pH towards the anode, achieving a total copper removal of 97.92%. These results highlight the critical role of optimizing both the electric current and the process duration to achieve the desired removal rates efficiently. In Exp8, the crosslinked sawdust/iron slag RFM-EK system achieved 26.72%, 54.36%, and 56.44% removal, respectively.

While EK tests with kaolinite achieved excellent removal of metal ions, the decontamination of real soils is far more complex due to the presence of organic matter, microbial activity, and mineralogy that can affect metal mobility and binding. These factors may reduce the decontamination efficiency by altering metal behavior. Since heavy metals removal from the soil is a dynamic process during the EK process, the efficiency of the EK will be affected by several factors, such as various in the pH of the soil and other organic and inorganic metal ions in the soil that may interfere with the removal of metal ions. Therefore, pilot-scale studies in heterogeneous soils are essential to assess the practical applicability of the EK-RFM system under realistic conditions.

3.4 Specific Energy Consumption

It is essential to determine the specific energy consumption (SEC) to evaluate the overall energy usage and treatment expenses, as described in Eq. 5. This equation computes the SEC across all experimental scenarios (Ghobadi et al., 2021a, 2021b). The fluctuations in the copper removal (Cu^{2+}) and the

corresponding energy requirement throughout the RFM-EK experiments are shown in Fig. 4c. These variations are illustrated across different experimental conditions in Table 2. The investigation examined how higher electrical current and extended processing time affect the removal rate of Cu^{2+} and energy consumption. A thorough examination of these factors was conducted, and their influence is depicted in Fig. 4c. Substantial Cu^{2+} removal was observed across all tests, and the power consumption analysis revealed a notable increase in energy requirements of the EK process when the electrical current changed from 20 to 30 mA in Exp3 to Exp5.

A comparison of Exp 3 and Exp 4 revealed a general increase in the removal rate of Cu^{2+} with the transition of the electrical current from 20 to 25 mA at the experiment's outset. Notably, the improvement in copper removal coincided with an energy consumption decrease from 0.153 kWh. Kg^{-1} to 0.145 kWh. Kg^{-1} . As the electrical current was increased to 30 mA in Exp5, the energy consumption reached 0.202 kWh/kg, with a slight increase in the Cu^{2+} removal from 88.1% in Exp4 to 88.91 in Exp5.

In contrast, the energy consumption in Exp6 conducted at 25 mA electric current was 0.146 kWh/kg, and total copper removal reached 90.30%. Results reveal that Exp6 achieved higher Cu^{2+} removal than Exp4, conducted at the same electric current, but energy consumption was the same in both experiments. Contrarily, the Cu^{2+} removal increased at 25 mA in Exp4 compared to 30 mA in Exp5; all was achieved at higher energy consumption (Fig. 4c). The higher SEC in Exp8 is attributed to the greater complexity of heavy metals removal from contaminated sites where soil heterogeneity, elevated organic content, and stronger metal-binding properties increase resistance to EK treatment, necessitating more energy to disrupt these bonds. The presence of competing ions and the longer treatment duration (35 days) further raised energy requirements, leading to a substantial SEC increase relative to kaolinite-based experiments.

3.5 Characteristics of RFM

Sawdust garners significant attention among agricultural byproducts due to its cost-effectiveness and remarkable efficacy in eliminating heavy metals from wastewater. Its composition, comprising cellulose,

lignin, and carboxyl groups, enhances its capacity to attract cations to its active sites, rendering it an intriguing candidate for water purification purposes. The heavy metals' adsorption onto sawdust follows the Freundlich or Langmuir isotherms, demonstrating the potential for adsorption in single-layer and multiple-layer arrangements. Typically, the adsorption mechanism on sawdust follows the pseudo-second-order kinetic model, indicating a chemisorption process (Meez et al., 2021). Treatment with glutaraldehyde crosslinks the hydroxyl groups in sawdust, enhancing its structural integrity, reducing biodegradability, and introducing aldehyde (-CHO) groups that further facilitate metal binding. Acid treatment, typically using dilute mineral acids, removes impurities, increases the surface area, and exposes more reactive sites on both sawdust and iron slag. These chemical modifications improve the material's porosity, surface reactivity, and overall metal uptake capacity, thereby increasing the effectiveness and durability of the RFM in copper removal. Moreover, iron slag exhibits notable features of excellent specific surface area and significant porosity, making it a cost-effective adsorbent for soil treatment. The efficacy of iron slag in metal ions removal depends on its distinctive properties and chemical composition (Ganbat et al., 2023; Hamdi et al., 2024). This investigation employed a blend of sawdust and iron slag RFM to maximize Cu^{2+} adsorption by the RFM. Lignin in the sawdust contains hydroxyl, carboxyl, and methoxy groups, which can act as binding sites for heavy metal ions through complexation. Interaction between copper and lignin can involve coordination between the metal ions and the oxygen atoms in the functional groups of lignin, forming complexes known as chelates. These chelates are typically more stable than simple ion interactions. Further, oxides and hydroxides functional groups in iron slag adsorb copper iron through electrostatic attraction and complexation reactions. Iron slag also induces copper precipitation due to its alkaline pH (Table 1).

Figure 5a displays the outcomes of X-ray diffraction (XRD) analysis regarding the iron slag's composition originating from the steel-making procedure. The data indicate that iron oxide is the primary component in the slag waste matrix. Iron oxide exhibits notable adsorption capabilities, effectively removing contaminants (Díaz-Piloneta et al., 2022). Although the specific mechanism by which heavy metals interact with iron oxide is still being studied, it is known that iron oxide

can bind to or adsorb these elements on its surface. This ability is attributed to iron oxide's inherent properties, including its infinitesimal particles and notable porous nature that provide a substantial surface area, making it a remarkable RFM. Heavy metal adsorption onto iron oxide is characterized by electrostatic interactions among the metal molecules, which are subsequently followed by developing inner-sphere Fe-carboxylate complexes via ligand exchange (Jain et al., 2018).

Figure 5b illustrates the FTIR spectra of untreated RFMs, iron-slag-treated RFM, sawdust/iron-slag-treated RFM, and treated sawdust/iron RFM. The FTIR bands of iron slag, sawdust/iron slag, treated sawdust/iron, and sawdust/iron slag with 2% glutaraldehyde before and after EK treatment showed comparable features. Nevertheless, the bands exhibited greater prominence in the sawdust/iron slag both before and after EK treatment, underscoring the considerable efficacy of EK-treated sawdust/iron slag in removing Cu^{2+} . Following EK tests, the FTIR bands of slag, sawdust/slag, and treated sawdust/slag (Fig. 5b) displayed peaks in 3787, 3743, 1603, and 1525 cm^{-1} regions, indicative of OH^- stretch. The band 3787 cm^{-1} showed diminished intensity in Exp2, although it exhibited similar stretching in most EK tests. The band 3743 cm^{-1} intensity, to some extent, increased after the EK treatment in Exp5 and Exp6, attributed to added OH^- groups introduced by the sawdust/slag, causing intensity changes. In all experiments, there was no observable alteration in this band when the soil was treated with sawdust or iron slag. Additionally, in Experiment 2 with iron slag RFM, the FTIR band at 1603 cm^{-1} decreased.

Figures 5c to 5x present the results of the scanning electron microscope (SEM) with energy-dispersive X-ray spectroscopy (EDS) analysis performed on various configurations of RFM, including iron slag, sawdust/iron slag, treated sawdust/iron slag, and sawdust/iron slag mixed with a 2% glutaraldehyde solution. These analyses were conducted before and after the EK treatment to examine the changes in surface morphology. In Fig. 5k, the SEM analysis of the iron slag RFM exhibits semi-smooth surfaces and solid structures after the EK treatment. In contrast, Figs. 5m to 5r display rougher surfaces for the sawdust/iron slag combination after the EK treatment. Figure 5s shows similar rough surfaces for the treated sawdust/iron slag. These observations suggest that the treatment led to an increase in the surface area of the sawdust/iron slag, thereby enhancing its sorption capacity. The rougher surface

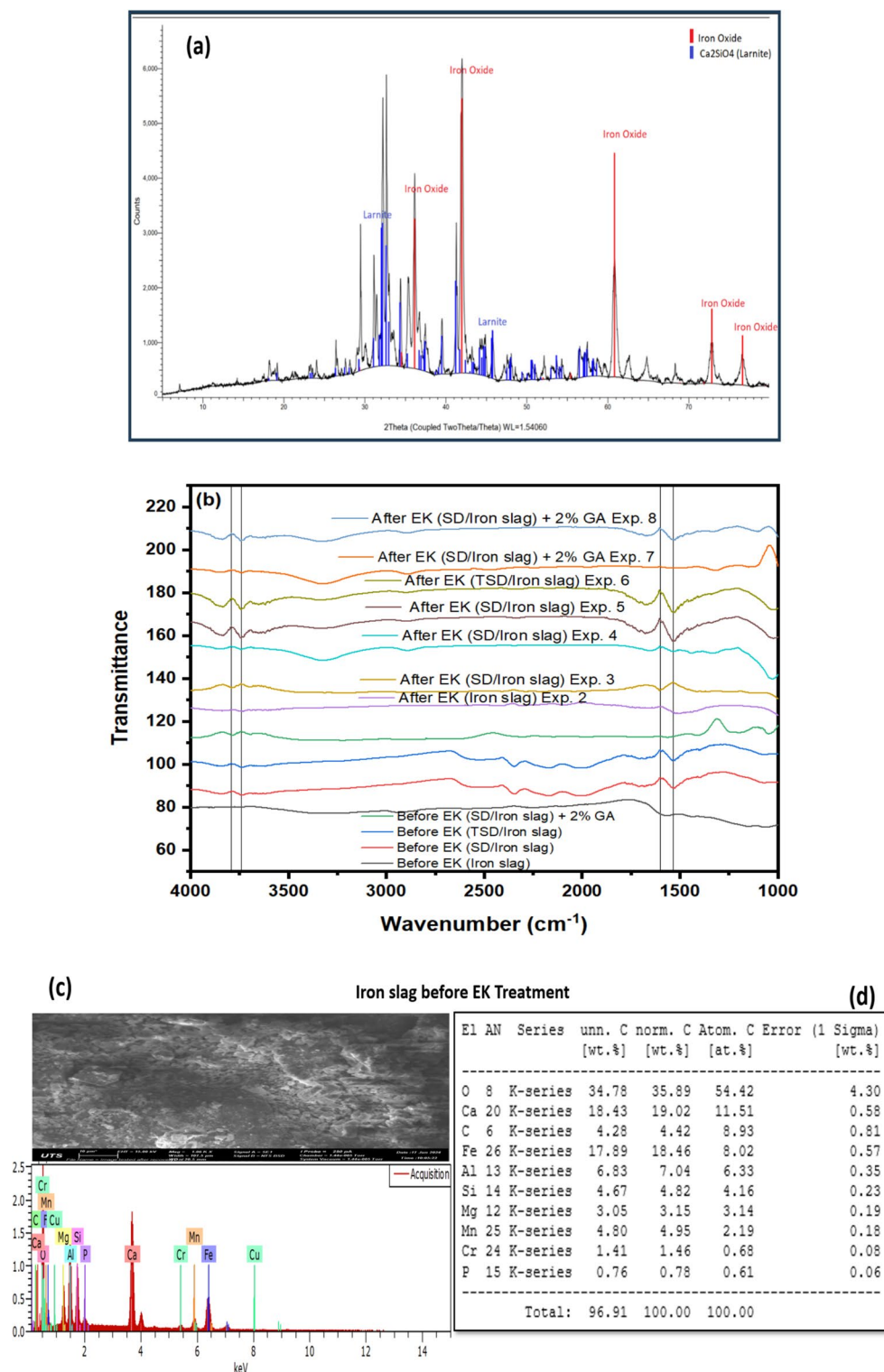


Fig. 5 (a) the XRD spectrum of iron slag, (b) FTIR bands of slag, SD/slag, TSD/iron slag, and SD/slag mix with 2% GA before and after EK treatment, and (c to x) slag, SD/slag, TSD/

slag, and SD/slag mix with 2% GA SEM images with EDS before and at the end of the EK treatment

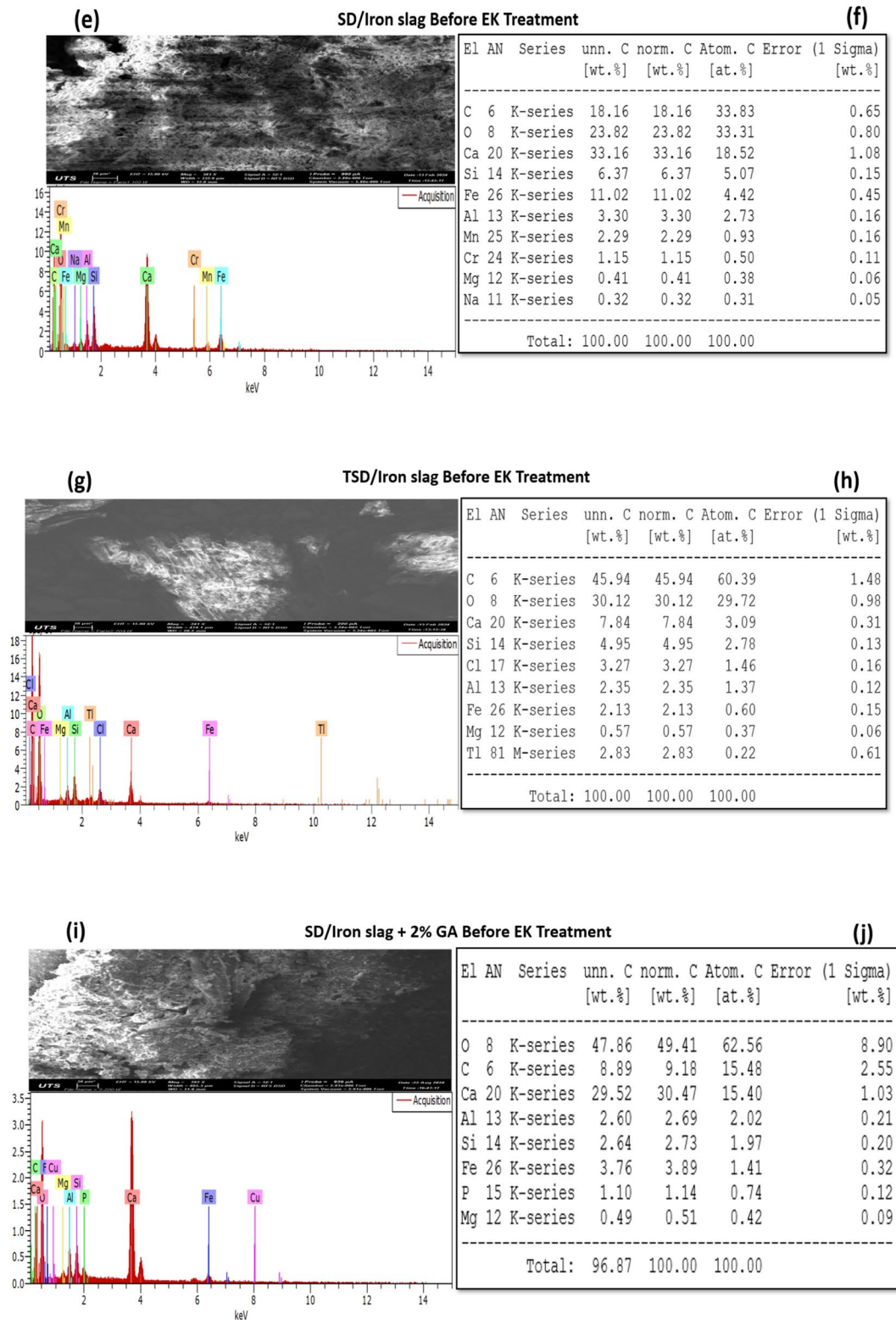


Fig. 5 (continued)

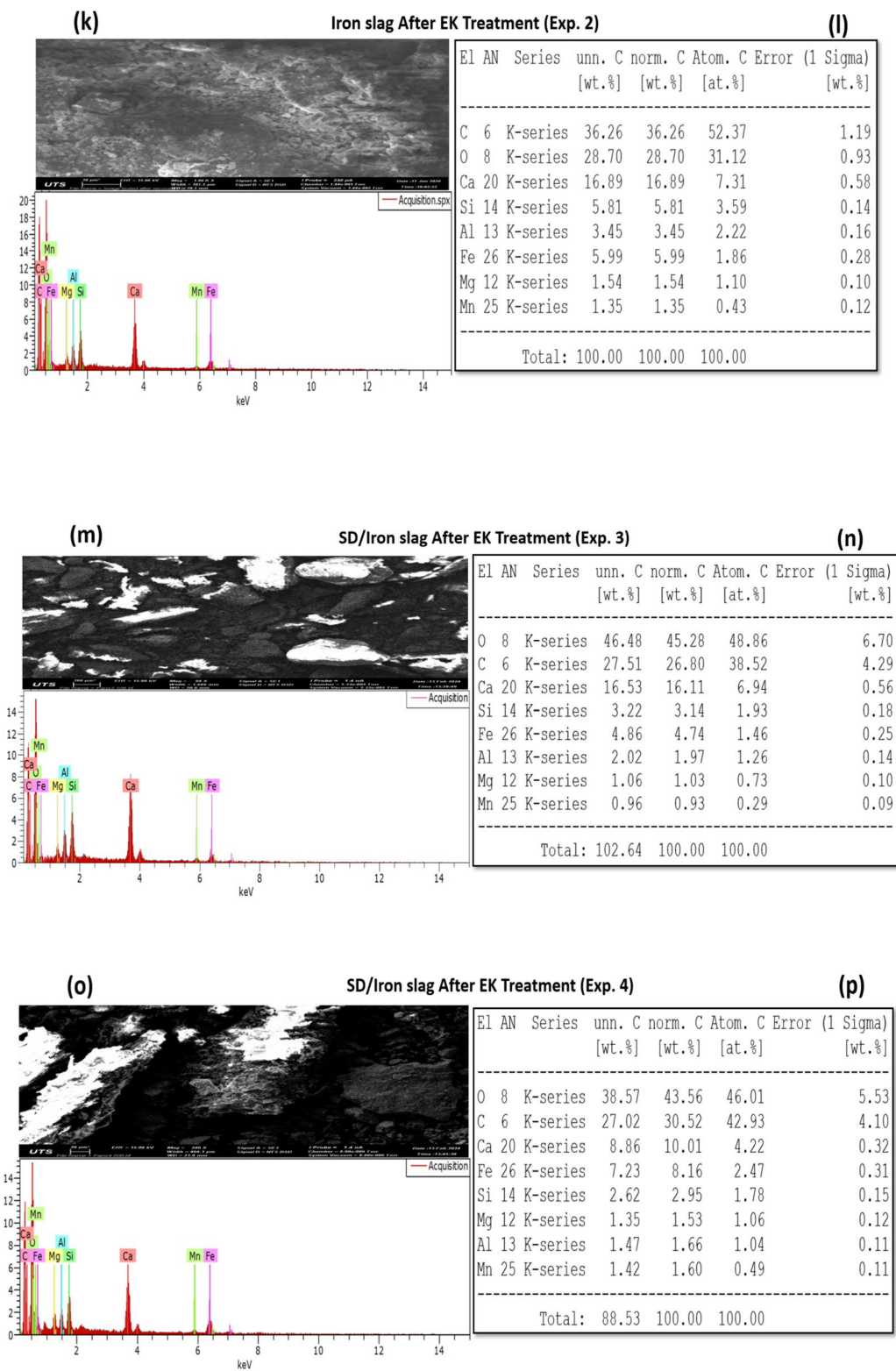


Fig. 5 (continued)

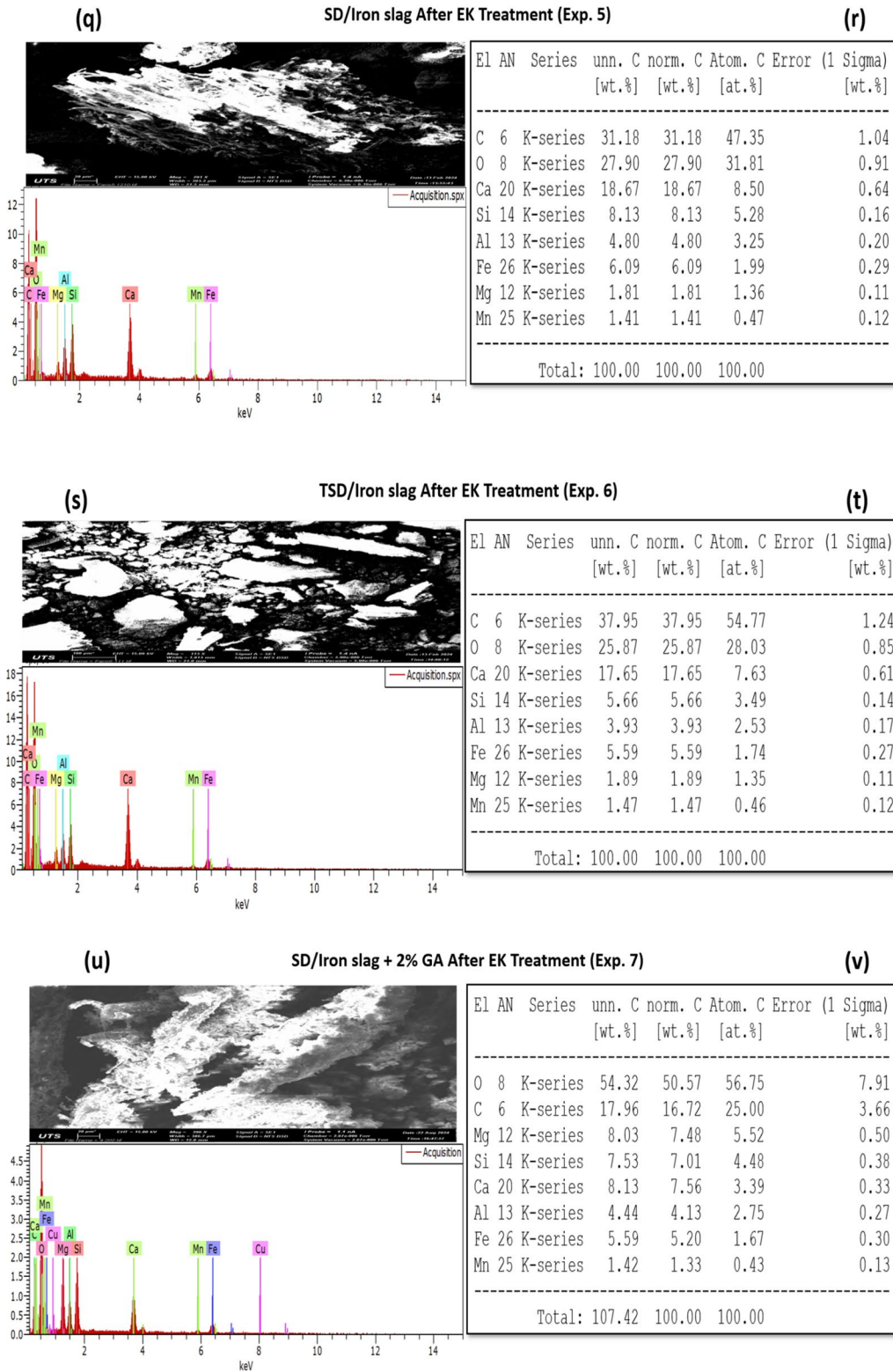


Fig. 5 (continued)

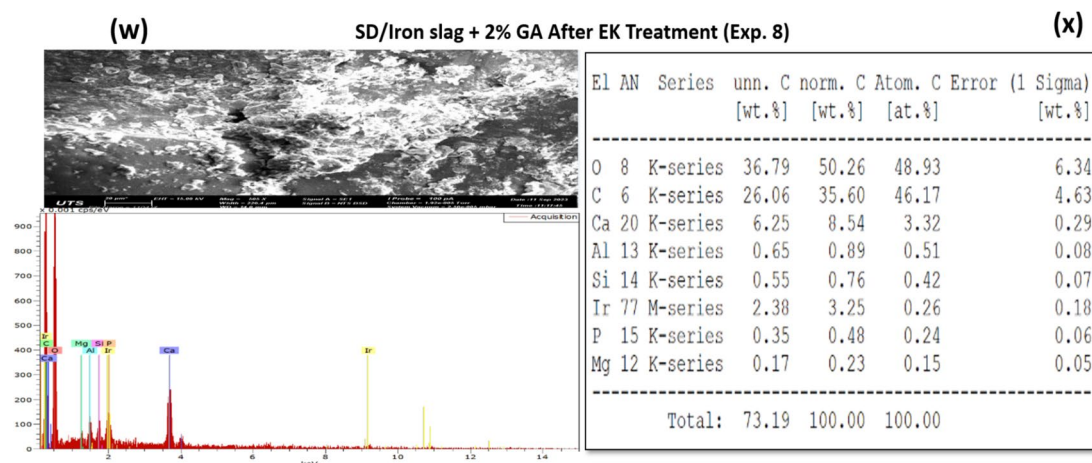


Fig. 5 (continued)

morphology indicates that the material's ability to adsorb contaminants was improved due to the increased surface area available for interaction. The treatment of sawdust/iron slag with 2% glutaraldehyde solution enhances its surface properties, making it more effective for contaminant adsorption. The aldehyde groups in glutaraldehyde likely react with functional groups on the sawdust and iron slag, such as hydroxyl and carboxyl groups, leading to cross-linking or chemical modification. This process can result in the formation of additional active sites and a more uniform surface morphology, as observed in Fig. 5u to 5x.

Generally, sawdust possesses a porous structure ideal for adsorption applications, enabling it to bind heavy metal ions effectively. Its efficacy as an adsorbent in heavy metal removal has been well-established in wastewater treatment (Božić et al., 2009; Meez et al., 2021). Sawdust is also characterized by its composition, which includes cellulose, lignin, and carboxyl groups, which enhances its ability to homogenize with iron slag. Iron slag also has features that contribute to the homogenization process, including its high surface area and extensive porosity. These properties make it a desirable choice as a material that can be homogenized with other materials. However, the introduction of 2% glutaraldehyde into sawdust and iron slag significantly improved the adsorption process and Cu^{2+} removal efficiency. The glutaraldehyde helped to form a more homogeneous and reactive composite material, which enhanced the adsorption capacities of the sawdust and iron slag, resulting in a more effective stabilization of

Cu^{2+} , thus increasing the overall efficiency of the electrical process comparatively. The comparative analysis confirmed that the glutaraldehyde-treated composite exhibited superior adsorption capacity compared to untreated combinations of sawdust and iron slag or their components. This indicates that glutaraldehyde not only enhances surface properties but also promotes synergistic effects within the composite, making it an effective solution for heavy metal remediation in EK systems, as observed in Fig. 6c. The glutaraldehyde also contributed to the pH reduction by crosslinking with the cellulose in the sawdust. This crosslinking process likely stabilizes the RFM mixture, thus reducing alkaline migration toward the anode and maintaining a lower pH throughout the experiment. This decrease in pH can be beneficial to enhance the removal of Cu^{2+} .

4 Implications

EK experiments demonstrated a great potential for using industrial waste materials as an adsorbent in copper removal from the soil. Copper removal from kaolinite soil was 3.21% in the EK process without RFM, then increased to 23.76% when iron slag RFM was coupled with the EK process. Although iron slag is a good adsorbent for heavy metals, it was unable to prevent the rapid advancement of OH^- in the soil due to its alkaline pH (Table 1). Therefore, most copper was precipitated in section S6, adjacent to the RFM in Exp2. Using sawdust-iron slag RFM in Exp3 increased

copper removal to 71.8%, with 67.7% of the copper captured by the RFM. Sawdust-iron slag RFM of pH 10.19 (Table 1) was able to suppress the advancement of OH^- in the soil, allowing copper transport toward the RFM. Treated sawdust-iron slag RFM of pH 9.24 (Table 1) further improved copper removal to 90.3%, with >84% of the copper captured in the RFM. In Exp7, the total copper removal efficiency increased to 97.92% with the incorporation of a 2% glutaraldehyde. This improvement is likely due to the enhanced properties of the RFM, which consisted of a mixture of sawdust and iron slag. The glutaraldehyde improved copper removal by modifying the cellulose structure in the sawdust and by reducing the pH of the RFM (Table 1). These modifications likely enhanced the RFM's effectiveness in adsorbing and removing contaminants during the electrokinetic process. The total removal efficiency in Exp8 using natural soil was lower compared to kaolin soil due to the inherent complexity of natural soil. Factors such as its heterogeneity, elevated organic matter content, and stronger metal-binding properties contribute to greater resistance to electrokinetic (EK) treatment, making the remediation process less effective. The results emphasize the potential of applying industrial waste materials as adsorbents in soil treatment, reducing the environmental impact, cost, and waste generation from the remediation process. Although EK requires low energy for operation, coupling the EK-RFM with solar energy will reduce the operation cost of the remediation process. The EK-RFM system will also reduce the human risk associated with conventional ex-situ remediation processes. Combining the EK with RFM will ensure not only better heavy metal removal but also easier heavy metal extraction and control since the relatively high permeability RFM will capture most contaminants at the end of the remediation process. The RFM-EK hybrid system will facilitate soil decontamination and resource recovery, encouraging more work on recycling waste materials for environmental remediation processes. It is noteworthy that the effectiveness of the RFM decreases at the end of the EK process due to the variation in the soil pH, affecting the functional groups of the FMS and its adsorption capacity. Also, the desorption process is carried out in an acidic environment that alters the surface characteristics and charge of the RFM media (Fig. 6c), rendering it less effective for use in multiple cycles (Ganbat et al., 2023; Hamdi et al., 2024).

5 Conclusion

Hybrid RFM consisting of organic and inorganic adsorbents was tested for heavy metals removal from kaolinite and contaminated site soil. Using recyclable and eco-friendly waste materials in the RFM aims to achieve sustainable land-remediation processes. Iron slag, iron slag/sawdust, and treated sawdust/iron slag were investigated for Cu^{2+} removal. Cu^{2+} removal rose from 3.21% in the EK process to 23.76% in the iron slag-EK test. The iron slag's alkaline pH promoted the adsorption and precipitation of copper ions. Still, most Cu^{2+} was found to be precipitated outside the RFM due to the rapid progression of the alkaline front in the soil. Cu^{2+} removal was significantly enhanced by combining the EK method with the sawdust-iron slag RFM, achieving a 71.80% removal. In Exp6, 90.30% copper removal was reached when RFM containing treated sawdust and iron slag was utilized. The glutaraldehyde crosslinked sawdust/iron slag RFM-EK system attained 97.92% Cu^{2+} removal efficiency from kaolinite soil. Glutaraldehyde crosslinker of pH 4 to pH 5 reduced the pH of the iron slag RFM from pH 11.38 in Exp 2 to pH 9.55 in Exp 7; hence, there is no need for further enhancement. In the natural soil, the removal rates were lower due to the complicated chemistry of natural soils and the interaction between pollutants and the soil's organic matter. Future research should focus on further improving the conditions of the RMF-EK system by optimizing the experimental conditions, including increasing the amount of RFM in the soil, test duration, and using chemical enhancement agents to prevent alkaline front advancement in soil. RFM-EK pilot plant tests are recommended in future work to confirm the technology's efficiency and cost-effectiveness in the real environment. The environmental impact of the EK process should also be evaluated to develop mitigation systems. For example, the electrokinetic process can cause substantial pH changes in the soil, which may mobilize other harmful metals or disrupt soil ecosystems. There is also a risk of secondary pollution from the improper disposal of spent RFM saturated with heavy metals. A thorough life cycle assessment (LCA) and cost-benefit analysis would be necessary to evaluate the method's sustainability and practical feasibility on an industrial scale.

Acknowledgements The author acknowledges the Ministry of Government of Saudi Arabia for granting scholarship assistance to Faris M. Hamdi.

Author Contribution Faris M. Hamdi: Conceptualization, Methodology, Formal analysis, Investigation, Data curation, Writing – original draft, Writing – review & editing. Ali Altaee: Conceptualization, Methodology, Formal analysis, Investigation, Writing – original draft, Writing – review & editing, Supervision. Yahia Aedan: Writing – review & editing. John Zhou: Formal analysis, Investigation. Maryam AL Ejji: Resources, Investigation. Alaa H. Hawari: Resources, Formal analysis. Syed Javaid Zaidi: Resources, Formal analysis. Marwa Mohsen: Writing – review & editing. Rokhsare Kardani: Writing – review & editing.

Funding Open Access funding enabled and organized by CAUL and its Member Institutions. This study received funding from a food security research grant (MME03-1015–210003) provided by the Qatar National Research Fund (QNRF), in collaboration with the Ministry of Municipality. The authors take full responsibility for the content of this work.

Data Availability All data obtained have been shared in the form of figures and tables.

Declarations

Conflict of interest The authors declare that they have no conflict of interest.

Appendix

RFM Adsorption/Desorption

Figures 6a and 6b illustrate the results of dynamic adsorption using a combination of sawdust and iron slag. A pseudo-second-order (PSO) adsorption model was employed to evaluate the adsorption of metal ions onto the surface of RFM. This model is based on the following assumptions: i) the adsorbent surface is homogeneous, ii) the adsorption of metal ions onto RFM is governed by chemisorption, and iii) the reaction rate depends on the availability of active sites. The Cu^{2+} behaviour during adsorption was thoroughly investigated, revealing that the highest adsorption capacity, reaching 26.66 mg/g Cu^{2+} , is achieved within 20 min using sawdust or HCl-treated sawdust combined with iron slag and sawdust/iron slag mix with 2% GA solution. At first, the absorption of Cu^{2+} happens swiftly, demonstrating a notable rate of adsorption. However, as equilibrium is approached, the adsorption and desorption rates gradually equalise. Variables such as the

contact duration and the distinct properties of the sawdust/slag blend influence the extent of Cu^{2+} adsorption and the absorption rate (Kulal & Badalamoole, 2020).

The slowing down of adsorbate interactions at specific sites compared to those in the bulk phase influenced the extraction rate. The speed at which adsorbate molecules were removed from the solution varied based on their movement in the adsorbent from the surface to the inside. Characterized by a balance between adsorption and desorption rates, equilibrium was achieved within 200 min for the Cu^{2+} (Rahchamani et al., 2011; Zhuang et al., 2016). The magnetite nanoparticles with embedded Fe^{2+} ions serve as electron donors (Castro et al., 2018). The primary techniques utilized for ions removal from solution include electrostatic adsorption, Cu^{2+} binding to surfaces of metal oxide, and ion exchange with H^+ from OH^- groups on the surface of the adsorbent, forming complexes. Adsorbents possessing various chemical functionalities like carboxyl, aldehyde, ester, hydroxyl, and ketone groups can interact with copper ions. The effectiveness of this interaction depends on variables such as the number of binding sites, accessibility, chemical structure, and the binding involved (Jain et al., 2018).

Three cycles of adsorption and desorption were conducted using a feed concentration of 2.52 g/L of Cu^{2+} ions, 24 h each cycle, aimed at evaluating the sequential removal process. Throughout the adsorption cycles, the removal percentages of Cu^{2+} ions from the initial content in sawdust/iron slag were 57%, 48.54%, and 41.94% in cycles 1 to 3. Similar results were obtained for sawdust/iron slag mix with 2% GA solution, with removal percentages of 58.54%, 48.60%, and 40.37% in cycles 1 to 3. Additionally, the desorption concentrations at the end of the three cycles were 50.22%, 39.96%, and 36.86% for sawdust/iron slag and 50.86%, 37.15%, and 35.59% for sawdust/iron slag with 2% GA (Fig. 6c). The desorption process of sawdust/slag includes the release of formerly bound molecules/ions, which occurs via various methods such as diffusion, exchange reactions, and solvent and external stimuli. Distribution occurs as adsorbed species move along concentration gradients, moving from areas of higher to lower concentrations. The exchange reactions substitute less tightly bound species with those that have a higher affinity, whereas solvents can modify the interactions involving sawdust/slag and the adsorbed species. Protons compete with binding sites in acidic

environments, deteriorating interactions and facilitating the release of adsorbed copper ions, highlighting the significance of solution conditions in desorption phenomena.

Adsorption experiments are being conducted to evaluate the potential for RFM reuse, revealing moderate to high recovery rates of adsorbed copper when using acid regeneration methods. Typically, dilute hydrochloric or nitric acid solutions can desorb 70–90% of the copper from the media, depending on contact time and acid concentration. However, repeated sorption–desorption cycles tend to degrade

the structural and chemical integrity of the materials. In sawdust, prolonged acid exposure may hydrolyze cellulose components or leach out functional groups, reducing its adsorption capacity. Iron slag may also undergo surface alterations, including dissolution or passivation of active sites. As a result, the performance of RFM generally diminishes after 3 to 5 cycles, beyond which the cost of regeneration may outweigh the benefits. While RFM can be reused to a certain extent, its service life is finite, and periodic replacement or supplementation with fresh media is necessary to maintain high removal efficiency.

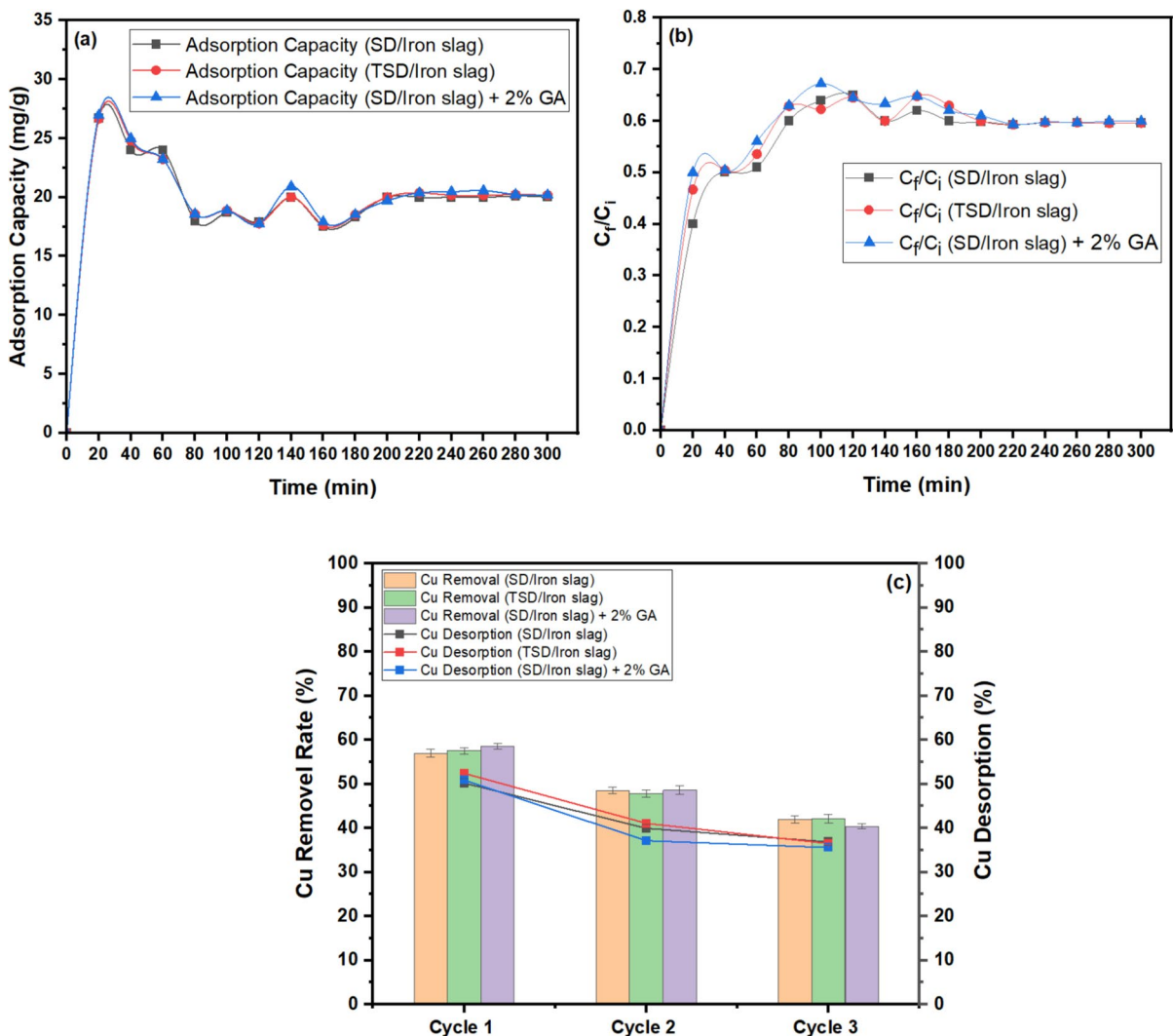


Fig. 6 Cu²⁺ adsorption tests, (a) The Cu²⁺ adsorption on sawdust/slag, (b) The influence of the duration on the Cu²⁺ adsorption, (c) Adsorption, and desorption of Cu²⁺ across

three successive cycles, sawdust (SD), treated sawdust (TSD) with slag, and sawdust/iron slag with 2% GA RFM

Open Access This article is licensed under a Creative Commons Attribution 4.0 International License, which permits use, sharing, adaptation, distribution and reproduction in any medium or format, as long as you give appropriate credit to the original author(s) and the source, provide a link to the Creative Commons licence, and indicate if changes were made. The images or other third party material in this article are included in the article's Creative Commons licence, unless indicated otherwise in a credit line to the material. If material is not included in the article's Creative Commons licence and your intended use is not permitted by statutory regulation or exceeds the permitted use, you will need to obtain permission directly from the copyright holder. To view a copy of this licence, visit <http://creativecommons.org/licenses/by/4.0/>.

References

- Altaee, A., Smith, R., & Mikhalovsky, S. (2008). The feasibility of decontamination of reduced saline sediments from copper using the electrokinetic process. *Journal of Environmental Management*, 88, 1611–1618. <https://doi.org/10.1016/J.JENVMAN.2007.08.008>
- Bahemmat, M., Farahbakhsh, M., & Kianirad, M. (2016). Humic substances-enhanced electroremediation of heavy metals contaminated soil. *Journal of Hazardous Materials*, 312, 307–318. <https://doi.org/10.1016/j.jhazmat.2016.03.038>
- Božić, D., Stanković, V., Gorgievski, M., Bogdanović, G., & Kovačević, R. (2009). Adsorption of heavy metal ions by sawdust of deciduous trees. *Journal of Hazardous Materials*, 171, 684–692. <https://doi.org/10.1016/j.jhazmat.2009.06.055>
- Castro, L., Blázquez, M. L., González, F., Muñoz, J. A., & Ballester, A. (2018). Heavy metal adsorption using biogenic iron compounds. *Hydrometallurgy*, 179, 44–51. <https://doi.org/10.1016/j.hydromet.2018.05.029>
- Díaz-Piloneta, M., Ortega-Fernández, F., Terrados-Cristos, M., & Álvarez-Cabal, J. V. (2022). Application of Steel Slag for Degraded Land Remediation. *Land (Basel)*, 11, 224. <https://doi.org/10.3390/land111020224>
- Fagnano, M., Agrelli, D., Pascale, A., Adamo, P., Fiorentino, N., Rocco, C., Pepe, O., & Venterino, V. (2020). Copper accumulation in agricultural soils: Risks for the food chain and soil microbial populations. *Science of the Total Environment*, 734, 139434. <https://doi.org/10.1016/J.SCITOTENV.2020.139434>
- Farhad, M., Noor, M., Yasin, M. Z., Nizamani, M. H., Turan, V., & Iqbal, M. (2024). Interactive Suitability of Rice Stubble Biochar and Arbuscular Mycorrhizal Fungi for Improving Wastewater-Polluted Soil Health and Reducing Heavy Metals in Peas. *Sustainability*, 16, 634. <https://doi.org/10.3390/su16020634>
- Frick, H., Tardif, S., Kandeler, E., Holm, P. E., & Brandt, K. K. (2019). Assessment of biochar and zero-valent iron for in-situ remediation of chromated copper arsenate contaminated soil. *Science of the Total Environment*, 655, 414–422. <https://doi.org/10.1016/J.SCITOTENV.2018.11.193>
- Fu, R., Wen, D., Xia, X., Zhang, W., & Gu, Y. (2017). Electrokinetic remediation of chromium (Cr)-contaminated soil with citric acid (CA) and polyaspartic acid (PASP) as electrolytes. *Chemical Engineering Journal*, 316, 601–608. <https://doi.org/10.1016/j.cej.2017.01.092>
- Ganbat, N., Altaee, A., Zhou, J. L., Lockwood, T., Al-Juboori, R. A., Hamdi, F. M., Karbassiyazdi, E., Samal, A. K., Hawari, A., & Khabbaz, H. (2022). Investigation of the effect of surfactant on the electrokinetic treatment of PFOA contaminated soil. *Environmental Technology and Innovation*, 28, 102938. <https://doi.org/10.1016/J.ETI.2022.102938>
- Ganbat, N., Hamdi, F. M., Ibrar, I., Altaee, A., Alsaka, L., Samal, A. K., Zhou, J., & Hawari, A. H. (2023). Iron slag permeable reactive barrier for PFOA removal by the electrokinetic process. *Journal of Hazardous Materials*, 460, 132360. <https://doi.org/10.1016/j.jhazmat.2023.132360>
- Ghobadi, R., Altaee, A., Zhou, J. L., Karbassiyazdi, E., & Ganbat, N. (2021a). Effective remediation of heavy metals in contaminated soil by electrokinetic technology incorporating reactive filter media. *Science of the Total Environment*, 794, 148668. <https://doi.org/10.1016/j.scitotenv.2021.148668>
- Ghobadi, R., Altaee, A., Zhou, J. L., McLean, P., Ganbat, N., & Li, D. (2021b). Enhanced copper removal from contaminated kaolinite soil by electrokinetic process using compost reactive filter media. *Journal of Hazardous Materials*, 402, 123891. <https://doi.org/10.1016/J.JHAZMAT.2020.123891>
- Ghobadi, R., Altaee, A., Zhou, J. L., McLean, P., & Yadav, S. (2020). Copper removal from contaminated soil through electrokinetic process with reactive filter media. *Chemosphere*, 252, 126607. <https://doi.org/10.1016/J.CHEMOSPHERE.2020.126607>
- Gholizadeh, M., & Hu, X. (2021). Removal of heavy metals from soil with biochar composite: A critical review of the mechanism. *Journal of Environmental Chemical Engineering*, 9, 105830. <https://doi.org/10.1016/J.JECE.2021.105830>
- Groenenberg, J. E., Römkens, P. F. A. M., Zomer, A. V., Rodrigues, S. M., & Comans, R. N. J. (2017). Evaluation of the Single Dilute (0.43 M) Nitric Acid Extraction to Determine Geochemically Reactive Elements in Soil. *Environmental Science and Technology*, 51, 2246–2253. <https://doi.org/10.1021/acs.est.6b05151>
- Hamdi, F. M., Altaee, A., Alsaka, L., Ibrar, I., Al-Ejji, M., Zhou, J., Samal, A. K., & Hawari, A. H. (2024). Iron slag/activated carbon-electrokinetic system with anolyte recycling for single and mixture heavy metals remediation. *Science of The Total Environment*, 930, 172516. <https://doi.org/10.1016/j.scitotenv.2024.172516>
- Han, J.-G., Hong, K.-K., Kim, Y.-W., & Lee, J.-Y. (2010). Enhanced electrokinetic (E/K) remediation on copper contaminated soil by CFW (carbonized food waste). *Journal of Hazardous Materials*, 177, 530–538. <https://doi.org/10.1016/j.jhazmat.2009.12.065>
- Hawal, L.H., saeed, K. abdulhussein, Al-Sulttani, A.O., 2023. Copper metal elimination from polluted soil by electrokinetic technique. *Environ Monit Assess* 195, 443. <https://doi.org/10.1007/s10661-023-11057-4>

- Hu, S., Lu, Y., Peng, L., Wang, P., Zhu, M., Dohnalkova, A.C., Chen, H., Lin, Z., Dang, Z., Shi, Z., 2018. Coupled Kinetics of Ferrihydrite Transformation and As(V) Sequestration under the Effect of Humic Acids: A Mechanistic and Quantitative Study. *Environ Sci Technol* acs.est.8b03492. <https://doi.org/10.1021/acs.est.8b03492>
- Jain, M., Yadav, M., Kohout, T., Lahtinen, M., Garg, V. K., & Sillanpää, M. (2018). Development of iron oxide/activated carbon nanoparticle composite for the removal of Cr(VI), Cu(II) and Cd(II) ions from aqueous solution. *Water Resour Ind*, 20, 54–74. <https://doi.org/10.1016/j.wri.2018.10.001>
- Kulal, P., & Badalamoole, V. (2020). Hybrid nanocomposite of kappa-carrageenan and magnetite as adsorbent material for water purification. *International Journal of Biological Macromolecules*, 165, 542–553. <https://doi.org/10.1016/j.ijbiomac.2020.09.202>
- Meez, E., Rahdar, A., & Kyzas, G. Z. (2021). Sawdust for the Removal of Heavy Metals from Water: A Review. *Molecules*, 26, 4318. <https://doi.org/10.3390/molecules26144318>
- Rahchamani, J., Mousavi, H. Z., & Behzad, M. (2011). Adsorption of methyl violet from aqueous solution by polyacrylamide as an adsorbent: Isotherm and kinetic studies. *Desalination*, 267, 256–260. <https://doi.org/10.1016/j.desal.2010.09.036>
- Turan, V., 2024. Bioremediation of Lithium and Nickel from Soil and Water, in: Lithium and Nickel Contamination in Plants and the Environment. *World Scientific*, pp. 219–230. https://doi.org/10.1142/9789811283123_0009
- Wen, D., Fu, R., & Li, Q. (2021). Removal of inorganic contaminants in soil by electrokinetic remediation technologies: A review. *Journal of Hazardous Materials*, 401, 123345. <https://doi.org/10.1016/j.jhazmat.2020.123345>
- Xue, F., Yan, Y., Xia, M., Muhammad, F., Yu, L., Xu, F., Shiao, Y., Li, D., & Jiao, B. (2017). Electro-kinetic remediation of chromium-contaminated soil by a three-dimensional electrode coupled with a permeable reactive barrier. *RSC Advances*, 7, 54797–54805. <https://doi.org/10.1039/C7RA10913J>
- Yeongkyoo, K. (2018). Effects of different oxyanions in solution on the precipitation of jarosite at room temperature. *Journal of Hazardous Materials*, 353, 118–126. <https://doi.org/10.1016/j.jhazmat.2018.04.016>
- Yu, X., Muhammad, F., Yan, Y., Yu, L., Li, H., Huang, X., Jiao, B., Lu, N., & Li, D. (2019). Effect of chemical additives on electrokinetic remediation of Cr-contaminated soil coupled with a permeable reactive barrier. *R Soc Open Sci*, 6, 182138. <https://doi.org/10.1098/rsos.182138>
- Yuan, L., Xu, X., Li, H., Wang, N., Guo, N., & Yu, H. (2016). Development of novel assisting agents for the electrokinetic remediation of heavy metal-contaminated kaolin. *Electrochimica Acta*, 218, 140–148. <https://doi.org/10.1016/J.ELECTACTA.2016.09.121>
- Zhuang, Y., Yu, F., Chen, J., & Ma, J. (2016). Batch and column adsorption of methylene blue by graphene/alginate nanocomposite: Comparison of single-network and double-network hydrogels. *Journal of Environmental Chemical Engineering*, 4, 147–156. <https://doi.org/10.1016/j.jece.2015.11.014>

Publisher's Note Springer Nature remains neutral with regard to jurisdictional claims in published maps and institutional affiliations.